Increasing the efficiency of homology-directed repair for CRISPR-Cas9-induced precise gene editing in mammalian cells

Chu, V.T., Weber, T., Wefers, B., Wurst, W., Sander, S., Rajewsky, K., Kuehn, R.

This is the final version of the accepted manuscript. The original article has been published in final edited form in:

Nature Biotechnology
2015 MAY ; 33(5): 543-548
doi: 10.1038/nbt.3198
Nature Publishing Group

Increasing the efficiency of homology-directed repair for CRISPR/Cas9-induced precise gene editing in mammalian cells

Van Trung Chu[1], Timm Weber[1], Benedikt Wefers[2,3], Wolfgang Wurst[2,3,4], Sandrine Sander[1], Klaus Rajewsky[1*], Ralf Kühn[1,2,5*]

1. Max-Delbrück-Center for Molecular Medicine, Berlin, Germany

2. Helmholtz Zentrum München, German Research Center for Environmental Health, Neuherberg, Germany

3. Deutsches Zentrum für Neurodegenerative Erkrankungen e. V., Munich, Germany

4. Munich Cluster for Systems Neurology (SyNergy), Ludwig-Maximilians-Universität München, Munich, Germany

5. Berlin Institute of Health, Kapelle-Ufer 2, Berlin, Germany

*corresponding authors

Manuscript correspondence
Ralf Kühn E-Mail: ralf.kuehn@mdc-berlin.de Phone: +49-30-9406-2832

Klaus Rajewsky E-Mail: Klaus.Rajewsky@mdc-berlin.de Phone: +49-30-9406-3630

Max-Delbrück-Centrum for Molecular Medicine, Robert-Rössle-Str. 10, Berlin, Germany

The insertion of precise genetic modifications by genome editing tools such as CRISPR-Cas9 is limited by the relatively low efficiency of homology-directed repair (HDR) compared with the higher efficiency of the non-homologous end joining (NHEJ) pathway. To enhance HDR, enabling the insertion of precise genetic modifications, we suppressed the NHEJ key molecules KU70, KU80 or DNA Ligase IV by gene silencing, the Ligase IV inhibitor SCR7 or the coexpression of adenovirus 4 E1B55K and E4orf6 proteins in a `traffic light´ and other reporter systems. Suppression of KU70 and DNA Ligase IV promotes the efficiency of HDR 4–5-fold. When co-expressed with the Cas9 system, E1B55K and E4orf6 improved the efficiency of HDR up to 8-fold and essentially abolished NHEJ activity in both human and mouse cell lines. Our findings provide useful tools to improve the frequency of precise gene modifications in mammalian cells.

The clustered, regularly interspaced, short palindromic repeats (CRISPRs)-Cas9 endonuclease represent a versatile tool for genome engineering, enabling the induction of site-specific genomic double-strand breaks (DSBs) by single guide RNAs (sgRNAs)[1]. In mammalian cells DSBs are mostly repaired by the non-homologous end joining (NHEJ) pathway[2,3], frequently leading to the loss of nucleotides from the DSB ends. This enables the efficient construction of knockout alleles through the induction of frameshift mutations[4]. By contrast, the alternative pathway of homology-directed repair (HDR) can be utilized for the introduction of precise genetic modifications such as codon replacements or reporter insertions by recombination with exogenous targeting vectors, serving as repair template[5]. We reasoned that the efficiency of HDR and thus the construction of precise genetic modifications could be boosted by the transient inhibition of NHEJ key molecules, similar to what has been observed for *Drosophila* embryos with a genetic DNA Ligase IV deficiency[6].

To quantitatively determine the outcome of CRISPR-induced DSB repair, we first generated human HEK293 cells with a `traffic light´ reporter[7] (TLR) vector integrated into the AAVS1 locus[8] (Fig. 1a). HEK293 cells were transfected with an AAVS1 targeting vector carrying the TLR insert and Cas9 and AAVS1-specific sgRNA expression plasmids (Supplementary Fig. 1.1). Upon selection and genotyping of transfected cells we obtained heterozygous ($AAVS1^{TLR/+}$) and homozygous ($AAVS1^{TLR/TLR}$) targeted clones harboring the TLR construct in the AAVS1 locus (Supplementary Fig. 1.2). The reporter includes a CAG promoter for expression of a nonfunctional green fluorescent (Venus) gene, disrupted by the replacement of codons 117 - 152 with target sequences from the mouse *Rosa26* and *Rab38* locus, followed by coding regions for a self-cleaving 2A peptide and a red fluorescent (TagRFP) gene in a reading frame shifted by 2 bp

(Supplementary Table 1). CRISPR/Cas9-induced DSBs in the target region that are repaired via NHEJ and cause deletions, shift the translation to the frame of the 2A-TagRFP in about 1/3 of the mutagenic NHEJ events which can then be detected in reporter cells by the expression of RFP (Fig. 1b). If an intact Venus coding region is provided as repair template, cells that repair the DSBs by HDR express Venus. For activation of the TLR reporter we designed two sgRNAs against the *Rosa26* target sequence, of whichsgRosa26-1 showed a higher activity to induce deletions in the endogenous locus of mouse NIH3T3 cells (Fig. 1c).

Next, we transfected AAVS1$^{TLR/+}$ cells with an expression vector for Cas9, blue fluorescent protein (BFP) and sgRosa26-1, together with a linearized Venus donor plasmid. 72h after transfection the cells were analyzed by FACS, gated for BFP$^+$ transfected cells, and the frequency of Venus$^+$ and of RFP$^+$ cells was determined. We observed 3% of RFP$^+$ and 5% of Venus$^+$ cells indicating NHEJ or HDR repair events respectively, as compared to 0.1% RFP$^+$ and 0.6% Venus$^+$ cells in a control lacking sgRosa26-1 (Fig. 1d). Of note, RFP$^+$ cells detected by the TLR assay represent only 1/3 of all mutagenic NHEJ events. Similar results were obtained with AAVS1$^{TLR/TLR}$ cells (Supplementary Fig. 1.3).

For suppression of key NHEJ pathway proteins[2,9] by short hairpin (sh) RNAs, we added a human H1 promoter to the sgRosa26-1/Cas9/BFP expression vector and inserted published shRNA sequences to knockdown KU70, KU80 or DNA Ligase IV. We first determined the extent of NHEJ suppression by transfection of AAVS1$^{TLR/+}$ cells with individual sgRosa26-1/Cas9/BFP-H1shRNA expression vectors in the absence of a repair template. 72h after transfection the samples were analyzed for RFP$^+$ cells in comparison to controls including a scrambled shRNA or lacking an shRNA. A substantially suppression of NHEJ repair was observed upon the individual or combined knockdown of KU70, KU80 or DNA Ligase IV (Fig. 1e and Supplementary Fig. 1.4). Similar results were obtained in AAVS1$^{TLR/TLR}$ cell lines by the knockdown of KU70, KU80 or DNA Ligase IV (Supplementary Fig. 1.4). The knockdown of Ligase IV reduced its protein level in transfected AAVS1^{TLR} (BFP$^+$) cells by 70% (Supplementary Fig. 1.5).

As additional approaches DNA Ligase IV inhibition we used the small molecule inhibitor SCR7[10] or the Adenovirus 4 (Ad4) E1B55K and E4orf6 proteins that mediate the ubiquitination and proteasomal degradation of DNA Ligase IV[11,12]. For the coexpression of Ad4 proteins, sgRosa26-1, Cas9 and BFP from a vector pair we linked the Ad4

E1B55K or the Ad4 E4orf6 gene via self-cleaving 2A peptide sequences to BFP (Fig. 1f). Mono- or biallelic AAVS1^{TLR} cell lines were transfected with either sgRosa26-1/Cas9/BFP expression vector in the presence or absence of SCR7 inhibitor or with both sgRosa26-1/Cas9/BFP/Ad4 plasmids. The presence of SCR7 reduced the fraction of RFP$^+$ cells in the BFP$^+$ population 4-fold whereas the coexpression of Ad4 proteins lead to an 8-fold reduction, compared to controls lacking inhibitor or Ad4 proteins (Fig. 1f and Supplementary Fig. 1.6). The coexpression of Ad4 proteins reduced the level of DNA Ligase IV protein in transfected AAVS1^{TLR} (BFP$^+$) cells by 93% (Supplementary Fig. 1.5). Overall, these results show that the NHEJ repair of CRISPR/Cas9 induced DSBs can be suppressed by targeting DNA Ligase IV using RNA interference, SCR7 or, most efficiently the Ad4 proteins.

To assess the effect of NHEJ suppression on HDR, AAVS1$^{TLR/+}$ cells were transfected with Venus repair template together with sgRosa26-1/Cas9/BFP vector (+/- SCR7) or with sgRosa26-1/Cas9/BFP vectors including either shRNA constructs targeting KU70, KU80, or DNA Ligase IV or the Ad4 proteins. After 72h the frequency of RFP$^+$ and Venus$^+$ cells within BFP$^+$ cells was analyzed by FACS (Fig. 2a, 2b, Supplementary Fig. 2.1). Venus$^+$ (HDR) cells increased from 5% for sgRosa26-1/Cas9/BFP alone, to 8 – 14 % in the presence of single shRNAs against KU70, KU80 or DNA Ligase IV, to 25% in the presence of shRNAs against KU70 and DNA Ligase IV or 1 μM of the inhibitor SCR7, and further to 36% upon the coexpression of the Ad4 proteins. Thus, HDR efficiency was enhanced up to 5-fold in the presence of KU70 and Ligase IV shRNAs or SCR7, and up to 7-fold by the Ad4 protein pair (Fig. 2c and Supplementary Fig. 2.2).

Titration of SCR7 on AAVS1$^{TLR/+}$ cells showed an optimal effect at 1 μM concentration (Supplementary Fig. 2.3). In the presence of two shRNAs, SCR7 or Ad4 proteins we noticed diminished fluorescence signals within the population of Venus$^+$ cells at 72h after transfection (Fig. 2a, Supplementary Fig. 2.1, 2.3c), indicating reduced Venus expression in cells undergoing NHEJ blockade, possibly caused by local chromatin remodeling through an extended DNA damage response[13,14]. However, Venus expression was normal in clones established from AAVS1$^{TLR/+}$ cells targeted in the presence of Ad4 proteins, indicating that this effect is only transient (Supplementary Fig. 2.3d). From the sample expressing the Ad4 proteins, Venus$^+$ cells were sorted, and we established 24 clones to confirm the integrity of the repaired TLR loci using PCR and sequence analysis (Supplementary Table 2). In contrast to the increase of Venus$^+$ cells, RFP$^+$ cells decreased from 3% in the controls to 1.7%, 1.4% or 0.6% in the presence of

shRNAs, SCR7 or Ad4 proteins, respectively (Fig. 2a, 2b). Whether the residual NHEJ activity relies on the KU/Ligase IV independent alternative end-joining mechanism[15] remains to be determined.

Assessing the influence of the lengths of homology regions of the repair template on HDR efficiency we generated donor templates with 3' homology regions shortened from 1450 bp as in the original donor template to 350 bp (Fig. 2d and Supplementary Fig. 2.4). We transfected AAVS1$^{TLR/+}$ cells with sgRosa26-1/Cas9/BFP expression vector and each of the various donor templates, with or without the coexpression of Ad4 proteins. FACS analysis revealed a reduced targeting frequency (2%) for the donor with a 350 bp 3`homology region whereas the other molecules showed HDR efficiencies in the range of 5% (Fig. 2e). In the presence of Ad4 proteins the frequency of Venus$^+$ cells increased robustly up to 25% for the 350 bp donor and to 30% for the other donor molecules. In line with the previous results, the frequency of RFP$^+$ cells was strongly reduced by the coexpression of Ad4 proteins (Fig. 2f). Thus, PCR generated fragments with combined homology regions of > 1 kb are effective donors for HDR (Fig. 2e, f and Supplementary Fig. 2.4).

Applying our approach to an endogenous genomic locus we inserted a GFP reporter gene into the *AAVS1* locus of HEK293 cells. The AAVS1-SA-T2A-GFP targeting vector includes AAVS1 homology regions flanking a splice acceptor site and a 2A peptide sequence linked to GFP, enabling reporter expression by the AAVS1-derived transcript (Fig. 2g). HEK293 cells were cotransfected with a sgAAVS1-1/Cas9/mCherry expression plasmid and the AAVS1-SA-T2A-GFP targeting vector, with or without coexpression of Ad4 proteins. 72h after transfection the mCherry$^+$ transfected population exhibited 8% GFP$^+$ cells upon expression of sgAAVS1-1/Cas9 alone whereas the coexpression of Ad4 proteins raised their frequency cells to 66% (Fig. 2h). Thus, in line with the TLR results, we observed a 8-fold stimulation of gene targeting at the *AAVS1* locus by the coexpression of Ad4 proteins. FACS sorting and cloning GFP$^+$ cells 48h after transfection, we found correct GFP gene integration in 45 of 48 samples (95%), but only in 60% of the clones derived from the sample without Ad4 proteins (Supplementary Fig. 2.5, Supplementary Table 3), the remaining cells presumably representing random integrants.

Coexpression of Ad4 proteins also promoted HDR efficiency in a mouse Burkitt lymphoma (BL) cell line containing an activated PI3 kinase α-subunit[16] linked to an IRES element and a GFP reporter in the *Rosa26* locus. We targeted the GFP using a specific

sgRNA and a promoterless donor vector replacing GFP by BFP (Fig. 2i). The fraction of BFP^+ cells reports on HDR efficiency and GFP negative cells indicate NHEJ-mediated deletion events. Mouse BL cells were electroporated with Cas9 and the BFP replacement vector alone or with sgGFP/Cas9 expression plasmid with or without the coexpression of Ad4 proteins. Electroporation with sgGFP and Cas9 led to a transfection efficiency of 40%, as determined by mCherry expression after 24h. About half of the transfected cells (22% in total) had lost GFP expression after 72h (Supplementary Fig. 2.6) and 10% of the GFP^- cells were BFP^+ (Fig. 2j). The addition of Ad4 proteins reduced transfection efficiency to 27%, but again about half of the transfected cells (14% in total) lost GFP expression after 72h (Supplementary Fig. 2.6). Notably, 50% of the GFP^- cells were now BFP^+ (Fig. 2j), indicating a 5-fold stimulation of HDR by Ad4 proteins.

To assess whether a point mutation can be corrected in a tumor cell line we reverted the T24P codon replacement in the *Foxo1* gene of mouse BL cells, which renders FOXO1 resistant to AKT dependent phosphorylation. We transfected BL cells with a mutation specific sgRNA and a second sgRNA recognizing the first intron, expression vectors for Cas9 and fluorescent reporters without or together with Ad4 proteins and a targeting vector containing the reverted codon 24 (and harboring a silent nucleotide replacement) and a puromycin resistance gene (Supplementary Fig 2.7). At day 2 transfected cells were isolated by FACS sorting, subjected to puromycin selection and 53 or 39 single cell-derived clones were established from the sample without or with coexpression of Ad4 proteins, respectively. Genotyping of these clones by PCR and sequence analysis showed that 43 of the 53 clones derived without Ad4 proteins were mutants, 33 of these were heterozygous and 10 clones (19%) were homozygous targeted. In the presence of Ad4 proteins we found that all 39 clones were targeted, 24 of these were heterozygous and 15 clones (38%) homozygous mutants. Thus, despite the expected high targeting rate achieved with a selectable donor vector, the coexpression of Ad4 proteins further increased the targeting efficiency to 100% and doubled the net yield of homozygous targeted clones.

In summary, we show that for CRISPR/Cas9-induced mutagenesis the suppression of the NHEJ key enzyme DNA Ligase IV is an effective way for engineering precisely targeted mutations into the genome of mammalian cells. The activity of Ligase IV can be blocked by gene silencing, small molecule inhibition or proteolytic degradation, offering diverse approaches for the optimal delivery into target cells. For the proteolytic degradation of DNA Ligase IV we selected the E1B55K and E4orf6 proteins of

Adenovirus 4, shown to exert minimal influence on other cellular substrates such as Mre11 or p53, which are co-targeted by many other serotypes[17]. Nevertheless, we cannot exclude that HDR stimulation by the Ad4 proteins is mediated by the combined suppression of DNA Ligase IV and other regulatory proteins. It could be of further interest to compare the effect on HDR by the E1B55K and E4orf6 proteins of additional adenoviral serotypes and species identified from humans[18] and other vertebrates[19]. Furthermore, the use of Ad4 proteins may be also beneficial for the construction of targeted mouse mutants, as recently shown for zygotes cultured in the presence of SCR7[20]. In populations of cells transfected with a sgRNA, Cas9 and Ad4 protein expression plasmids we presently reach knock-in frequencies of up to 50 – 66%. By delivering Cas9 and of sgRNAs as synthetic RNAs it may be possible, as shown for human iPS cells[21], to further enhance gene targeting efficiencies. It will be interesting to apply CRISPR/Cas9 mutagenesis combined with NHEJ suppression also to early embryos of other model organisms and to primary mammalian cells to achieve gene corrections.

Acknowledgements

We thank K. Petsch and H. P. Rahn from the FACS core facility for excellent technical support. This work was supported by the European Research Council (ERC advanced grant ERC-AG-LS6, to K.R.), the German Ministry of Education and Research within the VIP program (TAL-CUT 03V0261, to W.W. and R.K.) and the European Union within the EUCOMMTOOLS project (FP7-HEALTH-F4-2010-261492, to W.W.)

Author contributions

V.T.C. K.R. and R.K. conceived and designed the project, V.T.C. and T.W. acquired the data, V.T.C., K.R, T.W. and R.K. analyzed and interpreted the data, B.W., S.S. and W.W. provided materials, V.T.C., K.R. and R.K wrote the paper.

Online Methods

Traffic light reporter construct The traffic light reporter (TLR) expression construct was assembled by cloning of PCR fragments encoding a defective venus (codons 117 – 152 replaced by a 52 bp segment derived from the mouse *Rosa26* locus (sgRNA target sequence underlined) and a 56 bp segment from the mouse *Rab38* gene) linked to the 2A peptide from Thosea asigna[22] and the coding region of TagRFP[23] in a 2 bp shifted reading frame (+3), cloned in between the CAG promoter and the polyA region of the bovine hGH gene. The CAG promoter was deleted from this plasmid to derive the traffic light targeting vector (Supplementary Table 1).

Cell culture and reagents Wild type, AAVS1^{TLR} HEK293, and mouse NIH3T3 cells were maintained in DMEM (Gibco) supplied with 15% FBS (Gibco), cells were passaged 3 times per week. The mouse Burkitt lymphoma cell line, generated from a Burkitt-like mouse lymphoma[16] was maintained in DMEM supplied with 15% FBS, 2mM HEPES (Gibco), 2mM Sodium Pyruvate (Gibco), 2mM L-Glutamine (Gibco), and 1x NAA (Gibco), beta-mercapthoethanol (Sigma) and passaged 4 times per week. For Puromycin selection, mCherry^{+} cells were sorted, seeded at 10^3 cells/well and selected with 3 μg/ml of Puromycin for 2 weeks. Then colonies were counted and single cell were sorted. The SCR7 inhibitor was purchased (Xcess Biosciences, San Diego, USA), 12h after transfection these cells were maintained in complete medium supplied with 1 μM

SCR7 inhibitor until analysis. At SCR7 concentrations of 60 μM and 10 μM we observed a reduction of transfection efficiency and of cell viability.

Donor vectors and CRISPR/Cas9-T2A-reporter vectors To generate the CRISPR/Cas9-T2A reporter vector, we amplified T2A-mCherry and T2A-BFP fragment by overlapping PCR and cloned them into FseI/EcoRI sites of plasmid pX330 (Addgene, #42230). The mCherry and BFP templates were derived from the plasmids MSCV-IRES-mCherry and MSCV-IRES-BFP, respectively, a kind gift of Frank Rosenbauer and Martin Janz (Charite, Berlin). To generate the AAVS1-SA-2A-Puro-TLR targeting vector, a CAG-Venus+1-P2A+3-mtagRFP+3 cassette was cloned into SalI/NotI sites of AAVS1-SA-2A-Puro targeting vector (Addgene, #22075). In addition, a SA-2A-GFP fragment was generated by overlapping PCR and inserted into the XhoI/SalI sites of the AAVS1 targeting vector, with the GFP template derived from a pRosa26-IRES-GFP plasmid (V.T.C., unpublished). For reporter replacement in the mouse cell line, the P110*-IRES-BFP-pA construct was generated by overlapping PCR and cloned into the pSTblue-1 sequencing plasmid (Novagen). For PCR donor templates, fragments were amplified with Herculase II Fusion DNA Polymerase (Agilent Technology) from pVenus+1-P2A+3-tagRFP plasmid using the same forward primer and different reverse primers (Supplementary Table 4).

Generation of CRISPR/Cas9 vector expressing shRNA or Ad4 proteins To generate CRISPR/Cas9-T2A-BFP/mCherry-hH1-shRNA vectors, the human H1 promoter and MCS sequence were generated by overlapping PCR and cloned into the NotI site of the CRISPR/Cas9-T2A-BFP/mCherry plasmid. To obtain CRISPR/Cas9-T2A-BFP/mCherry-P2A-Ad E1B55K or E4orf6 plasmids, the coding regions for adenoviral serotype 4 proteins were synthesized as mammalian codon optimized sequences (Supplementary Table 1) by Genscript (Piscataway, NJ, USA). Using these genes and BFP and mcherry template plasmids we amplified BFP/mCherry-P2A-Ad4 E1B55K and BFP/mCherry-P2A-Ad4 E4orf6 fragments and cloned them into the NheI/EcoRI sites of the CRISPR/Cas9-T2A-reporter plasmid by Gibson assembly (New England Biolabs, E2611S).

Single guide RNA and short hairpin shRNAs sgRNAs were designed based on unique sequences with 20 nt and as the last nucleotide before the PAM signal an A or G

was selected. The target sequences should hybridize with the sgRNA scaffold only at low energy as predicted by the Mfold web server (http://mfold.rna.albany.edu/?q=mfold/rna-folding-form). Complementary oligo-nucleotides were ordered separately, annealed, phosphorylated and cloned into the BbsI sites of the CRISPR/Cas9-T2A-reporter plasmid (Supplementary Table 4). For shRNA silencing, shRNA-targeted sequences were selected from previous reports[24,25,26,27,28,29] (Supplementary Table 4). Complementary oligonucleotides were ordered separately, annealed, phosphorylated and cloned into the BamHI/AflII sites of the CRISPR/Cas9-T2A-reporter-hH1 plasmid.

Transfection and Electroporation Human HEK293 and mouse NHI3T3 cells were plated into 24 well or 6 well plates at 1 day before transfection. At the day of transfection, these cells were supplied with new complete medium and the DNA mixed with FuGENE® HD Reagent (Promega) in Opti-MEM (Invitrogen) according to the manufacturer's introduction. After 15 minutes of incubation at RT, the mixture was dropped slowly into the well. For electroporation, mouse BL cells were harvested and counted, 1-2x10^6 cells resuspended with 3 μg plasmid DNA in 100 μl electroporation buffer and transferred to a 0.2 cm cuvette (Sigma) and electroporated using a Nucleofactor device (Lonza). Then, cells were transferred into pre-warmed complete medium.

Cell sorting and flow cytometry For single cell cloning, single cells were sorted into 96 well plates with 150 μl complete medium supplied with 10 μg/ml Gentamycin (Lonza). These plates were briefly centrifuged and incubated at 37^0C, 5% CO_2, the single cell clones were evaluated 3 days after sorting to exclude multiple cell contamination. Cells were cultured until confluence and duplicated for genotyping PCR. For the bulk sorting, the reporter$^+$ cells were sorted into 15 ml Falcon tubes with complete medium, cells were centrifuged and further cultured or used for the isolation of genomic DNA. For flow cytometry analysis, HEK293 cells were trysinized and resuspended in PBS/1% BSA FACS buffer and analysed with a Fortessa machine (Becton Dickinson). Mouse BL cells were harvested, centrifuged and resuspended in PBS/1% BSA FACS buffer.

Genomic DNA isolation, PCR and T7EI assay Reporter$^+$ cells were cultured and

harvested at different time points. Single cell clones were duplicated in 96 well plates. Genomic DNA was extracted using the QuickExtract DNA extraction kit (Epicentre) following the manufacturer's instruction. For T7EI assay, PCR was done using Herculase II Fusion DNA Polymerase (Agilent Technology) with PCR gene-specific primers (Supplementary Table 4) using the following conditions: 98^0C for 3 min; 35-37 cycles (95^0C for 20s, 60^0C for 20s, 72^0C for 20s) and 72^0C for 3 min. PCR products were run on 2% agarose gels, purified, denatured, annealed, and treated with T7EI (New England Biolabs). Cleaved DNA fragments were separated on 2% agarose gels and the DNA concentration of each band was quantified using the ImageJ software. Percent values of indels were calculated as described [30]. For genotyping PCR, genomic DNA was amplified using DreamTaq DNA Polymerase (Thermo Scientific) with primers listed in Supplementary Table 4.

DNA sequencing PCR products were directly sequenced by specific primers or cloned into the pSTBlue-1 Blunt vector (Novagen) following the manufacturer's protocol. Plasmid DNAs were isolated using the NucleoSpin Plasmid (Macherey-Nagel). Plasmids were sequenced using T7 forward primer (5'-TAATACGACTCACTATAGGG-3') by the Sanger method (LGCgenomics, Berlin,Germany).

Western blot analysis

Transfected AAVS1^{TLR} Reporter (BFP$^+$) cells were isolated by FACS and 10 x10^6 cells were lysed on ice in RIPA buffer (20 mM Tris-HCl [pH 7.5], 150mM NaCl, mM EDTA, 1% NP-40, 0.1% SDS, 0.1% sodium deoxycholate) for 20-30 min in the presence of protease inhibitors (Roche). The whole cell lysates were centrifuged for 10 min at 14.000 rpm. The supernatants were transferred into new tubes and protein concentrations were determined using the BCA protein assay (Biorad). The lysates were boiled at 100^0C for 5 min and loaded on SDS-PAGE gels. Blots were probed with anti-DNA ligase IV (H-300, Santa Cruz Biotechnology) and anti-beta-actin (AC-74, Sigma) antibodies. Blots were developed with secondary goat anti-rabbit IgG HRP (Southern Biotech) or anti-mouse IgG HRP (Southern Biotech) and bands visualised using the ECL detection kit (GE Healthcare).

References

1. Hsu, P. D., Lander, E. S. & Zhang, F. Development and applications of CRISPR-Cas9 for genome engineering. *Cell* **157,** 1262–1278 (2014).
2. Lieber, M. R. The mechanism of double-strand DNA break repair by the nonhomologous DNA end-joining pathway. *Annu. Rev. Biochem.* **79,** 181–211 (2010).
3. Mao, Z., Bozzella, M., Seluanov, A. & Gorbunova, V. Comparison of nonhomologous end joining and homologous recombination in human cells. *DNA Repair* **7,** 1765–1771 (2008).
4. Shalem, O. *et al.* Genome-scale CRISPR-Cas9 knockout screening in human cells. *Science* **343,** 84–87 (2014).
5. San Filippo, J., Sung, P. & Klein, H. Mechanism of eukaryotic homologous recombination. *Annu. Rev. Biochem.* **77,** 229–257 (2008).
6. Bozas, A., Beumer, K. J., Trautman, J. K. & Carroll, D. Genetic analysis of zinc-finger nuclease-induced gene targeting in Drosophila. *Genetics* **182,** 641–651 (2009).
7. Certo, M. T. *et al.* Tracking genome engineering outcome at individual DNA breakpoints. *Nat. Methods* **8,** 671–676 (2011).
8. Samulski, R. J. *et al.* Targeted integration of adeno-associated virus (AAV) into human chromosome 19. *EMBO J.* **10,** 3941–3950 (1991).
9. Panier, S. & Durocher, D. Push back to respond better: regulatory inhibition of the DNA double-strand break response. *Nat. Rev. Mol. Cell Biol.* **14,** 661–672 (2013).
10. Srivastava, M. *et al.* An inhibitor of nonhomologous end-joining abrogates double-strand break repair and impedes cancer progression. *Cell* **151,** 1474–1487 (2012).
11. Cheng, C. Y. *et al.* The E4orf6/E1B55K E3 ubiquitin ligase complexes of human adenoviruses exhibit heterogeneity in composition and substrate specificity. *J. Virol.* **85,** 765–775 (2011).
12. Forrester, N. A. *et al.* Serotype-specific inactivation of the cellular DNA damage response during adenovirus infection. *J. Virol.* **85,** 2201–2211 (2011).

13. Adam, S. & Polo, S. E. Blurring the line between the DNA damage response and transcription: the importance of chromatin dynamics. *Exp. Cell Res.* **329,** 148–153 (2014).
14. Zhu, Q. & Wani, A. A. Histone modifications: crucial elements for damage response and chromatin restoration. *J. Cell. Physiol.* **223,** 283–288 (2010).
15. Frit, P., Barboule, N., Yuan, Y., Gomez, D. & Calsou, P. Alternative end-joining pathway(s): bricolage at DNA breaks. *DNA Repair* **17,** 81–97 (2014).
16. Srinivasan, L. *et al.* PI3 kinase signals BCR-dependent mature B cell survival. *Cell* **139,** 573–586 (2009).
17. Cheng, C. Y. *et al.* The E4orf6/E1B55K E3 ubiquitin ligase complexes of human adenoviruses exhibit heterogeneity in composition and substrate specificity. *J Virol* **85,** 765–75
18. Ghebremedhin, B. Human adenovirus: Viral pathogen with increasing importance. *Eur. J. Microbiol. Immunol.* **4,** 26–33 (2014).
19. Benkő, M. *et al.* in *Virus Taxonomy, Eighth Report of the International Committee on Taxonomy of Viruses* 213–228 (Elsevier Academic Press, 2005).
20. Singh, P., Schimenti, J. C. & Bolcun-Filas, E. A mouse geneticist's practical guide to CRISPR applications. *Genetics* **199,** 1–15 (2015).
21. González, F. *et al.* An iCRISPR platform for rapid, multiplexable, and inducible genome editing in human pluripotent stem cells. *Cell Stem Cell* **15,** 215–226 (2014).
22. Donnelly, M. L. *et al.* The 'cleavage' activities of foot-and-mouth disease virus 2A site-directed mutants and naturally occurring '2A-like' sequences. *J. Gen. Virol.* **82,** 1027–1041 (2001).
23. Merzlyak, E. M. *et al.* Bright monomeric red fluorescent protein with an extended fluorescence lifetime. *Nat. Methods* **4,** 555–557 (2007).
24. Martinez, J. J., Seveau, S., Veiga, E., Matsuyama, S. & Cossart, P. Ku70, a component of DNA-dependent protein kinase, is a mammalian receptor for Rickettsia conorii. *Cell* **123,** 1013–1023 (2005).
25. Com, E. *et al.* Nerve growth factor receptor TrkA signaling in breast cancer cells involves Ku70 to prevent apoptosis. *Mol. Cell. Proteomics MCP* **6,** 1842–1854 (2007).
26. Li, B., Reddy, S. & Comai, L. Depletion of Ku70/80 reduces the levels of extrachromosomal telomeric circles and inhibits proliferation of ALT cells. *Aging* **3,** 395–406 (2011).

27. Munakata, Y. *et al.* Ku80 autoantigen as a cellular coreceptor for human parvovirus B19 infection. *Blood* **106,** 3449–3456 (2005).
28. Muylaert, I. & Elias, P. Knockdown of DNA ligase IV/XRCC4 by RNA interference inhibits herpes simplex virus type I DNA replication. *J. Biol. Chem.* **282,** 10865–10872 (2007).
29. Windhofer, F., Wu, W. & Iliakis, G. Low levels of DNA ligases III and IV sufficient for effective NHEJ. *J. Cell. Physiol.* **213,** 475–483 (2007).
30. Cong, L. *et al.* Multiplex genome engineering using CRISPR/Cas systems. *Science* **339,** 819–823 (2013).

Figure Legends

Figure 1 Insertion of a traffic light reporter into the *AAVS1* locus of HEK293 cells and suppression of the NHEJ pathway. **(a)** Strategy for insertion of the TLR construct into the *AAVS1* locus using CRISPR/Cas9 in human HEK293 cells. In the targeted sequence, the AAVS1-specific sgRNA is indicated in blue and the PAM signal is shown in red. The pAAVS1-TLR targeting vector includes homology arms (HA) of 800 bp flanking a splice acceptor (SA)-2A-Puromycin element and the traffic light reporter insert comprising a CAG promoter, a Venus gene inactivated by the replacement of 36 codons with target sequences from the mouse Rosa26/Rab38 loci (black insert). (**b**) Diagram of the TLR system. CRISPR/Cas9-induced DSBs in the target region, repaired via NHEJ resulting into deletions that shift translation by 2 bp, lead to RFP expression. An intact Venus coding region serves as repair template for HDR, leading to Venus expression. (**c**) Strategy to target the human *AAVS1*^{TLR} locus. Two different protospacers targeting the mouse *Rosa26-derived* sequence that interrupts the Venus gene are indicated in blue, with PAM signals in red. Empty vectors or sgRosa26-1 or sgRosa26-2/Cas9-T2A-mCherry expressing vectors were transfected into NIH3T3 cells to test cutting efficiency in the endogenous *Rosa26* locus. 48h after transfection, mCherry^{+} cells were sorted and PCR and T7EI assays performed. The percentage of indels was quantified by the ImageJ software. (**d**) AAVS1^{TLR} cells were cotransfected with linearized Venus repair vector and Cas9/BFP expression plasmids with or without (-) sgRosa26-1. 72h after transfection, flow cytometric analysis of BFP^{+} gated cells displayed 5% of Venus^{+} (HDR repair) cells and 3% of RFP^{+} (NHEJ repair) cells. The graphs represent triplicate data from 1 of 3 independent experiments with similar results, shown as mean ± SD. (**e**) Inhibition of the NHEJ pathway using gene silencing. Scheme of the sgRosa26-1/Cas9-2A-BFP-H1shRNA expression vector. AAVS1^{TLR} cells were transfected with sgRosa26-1/Cas9-2A-BFP (-) or sgRosa26-1/Cas9-2A-BFP-H1-shScrambled, -shKU70, -shLIG4 or -shKU70 or -shLIG4. 3 days later, these cells were analyzed by flow cytometry, gating on BFP^{+} transfected cells, and the percentage of RFP^{+} cells was determined. The graphs represent triplicate data from 1 of 3 independent experiments with similar results, shown as mean ± SD. (**f**) Suppression of NHEJ repair using the Ligase IV inhibitor SCR7 or the coexpression of Ligase IV degrading Ad4 E1B55K and E4orf6 (Ad4s) proteins. AAVS1^{TLR} cells were transfected with sgRosa26-1/Cas9-2A-BFP expression vector (-) or transfected and cultured with SCR7 or were transfected with the sgRosa26-1/Cas9-2A-

BFP-Ad4-E1B55K or -E4orf6 expression vectors. The samples were analyzed 3 days later by flow cytometry, gating on the BFP^+ transfected cells, and the percentage of RFP^+ cells was determined. The graphs represent triplicate data from 1 of 6 independent experiments with similar results, shown as mean ± SD. Significance was calculated using the Student t-test: ** $P < 0.01$, *** $P < 0.001$, ns – not significant.

Figure 2 Enhancement of HDR for CRISPR/Cas9-induced precise gene targeting. (**a**) Improvement of HDR efficiency by suppression of NHEJ key molecules. $AAVS1^{TLR}$ cells were cotransfected with linearized Venus repair vector and sgRosa26-1/Cas9/BFP expression plasmid together with shRNA cassettes, SCR7 inhibitor or the Ad4 E1B55K/E4orf6 proteins. The frequency of RFP^+ and $Venus^+$ cells within the transfected BFP^+ population was determined by flow cytometry. The data represent one of four independent experiments with similar results. (**b**) The graph summarizes the frequency of RFP^+ (red bars, significance compared to the (-) sample) and of $Venus^+$ (green bars; significance compared to the (-) sample) cells determined as in Fig. 2a. The y axis is represented as log10 scale. The bars represent mean values ± SD. (**c**) Relative increase of HDR efficiency (significance compared to the (-) sample) and of NHEJ suppression normalized to the control transfected with sgRosa26-1/Cas9 and targeting vector alone (-). The dotted line indicates a more than 2-fold increase of HDR. The bars represent mean values ± SD. (**d**) Use of PCR generated donor templates. Scheme of the TLR construct and of PCR donor fragments, having a constant 5' homology region of 400 bp whereas the length of the 3' homology region varies from 350 bp to 1250bp; as control the linearized promoterless Venus repair vector was used. (**e**) $AAVS1^{TLR}$ cells were cotransfected with sgRosa26-1/Cas9/BFP expression vector, the same molar amounts (800 fmol) of PCR donors or linearized Venus repair vector without or together with Ad4 E1B55K/E4orf6 proteins. The percentage of $Venus^+$ and RFP^+ cells was analyzed by flow cytometry 3 days after transfection. (**f**) The graph summarizes the frequency of RFP^+ (red bars) and $Venus^+$ (green bars) cells determined as in Fig. 2e. The data represent one of two independent experiments with similar results. The bars represent mean values ± SD. (**g**) Strategy for insertion of a GFP reporter gene into the human *AAVS1* locus using CRISPR/Cas9 in human HEK293 cells. The CRISPR/Cas9-targeted site is shown in Fig. 1a, in the AAVS1-GFP targeting vector the GFP gene is flanked by AAVS1 homology regions of 800 bp. (**h**) HEK293 cells were cotransfected with linearized AAVS1-GFP targeting vector and with sgAAVS1-1/Cas9/mCherry expression

vector or with sgAAVS1-1/Cas9/ mCherry-Ad4-E1B55K and -E4orf6 expression vectors. At day 3, the frequency of GFP^+ cells within the population of mCherry+ transfected cells was analyzed using the flow cytometric data; shown is one of triplicate samples obtained from one of two independent experiments. (**i**) Fluorescent reporter replacement in the mouse BL cell line. The cell line harbors an activated PI3 kinase (P110*)-IRES-GFP-pA cassette in the *Rosa26* locus. In the targeted GFP sequence, the sgGFP target sequence is highlighted in blue and the PAM element in red. DSBs repaired via the NHEJ pathway lead to the inactivation of GFP. DSBs repaired via HDR with the pBFP donor template lead to the replacement of GFP by the BFP reporter gene. (**j**) Mouse BL cells were electroporated with Cas9/mCherry or sgGFP/Cas9/mCherry expression vector and the pBFP donor plasmid without or together with coexpression of the Ad4 E1B55K/E4orf6 proteins. The frequency of GFP^-BFP^- (white bars) and GFP^-BFP^+ (blue bars) cells was analyzed at day 3. The graph summarizes triplicate results from one of three independent experiments with similar results. The bars represent mean values ± SD. Significance was calculated using the Student t-test: ** $P < 0.01$, *** $P < 0.001$, **** $P < 0.0001$, ns – not significant.

Competing financial interests

R.K. and W.W. are inventors on a patent application entitled `Improved recombination efficiency by inhibition of NHEJ DNA repair´ (EP2718446).

Figure 1

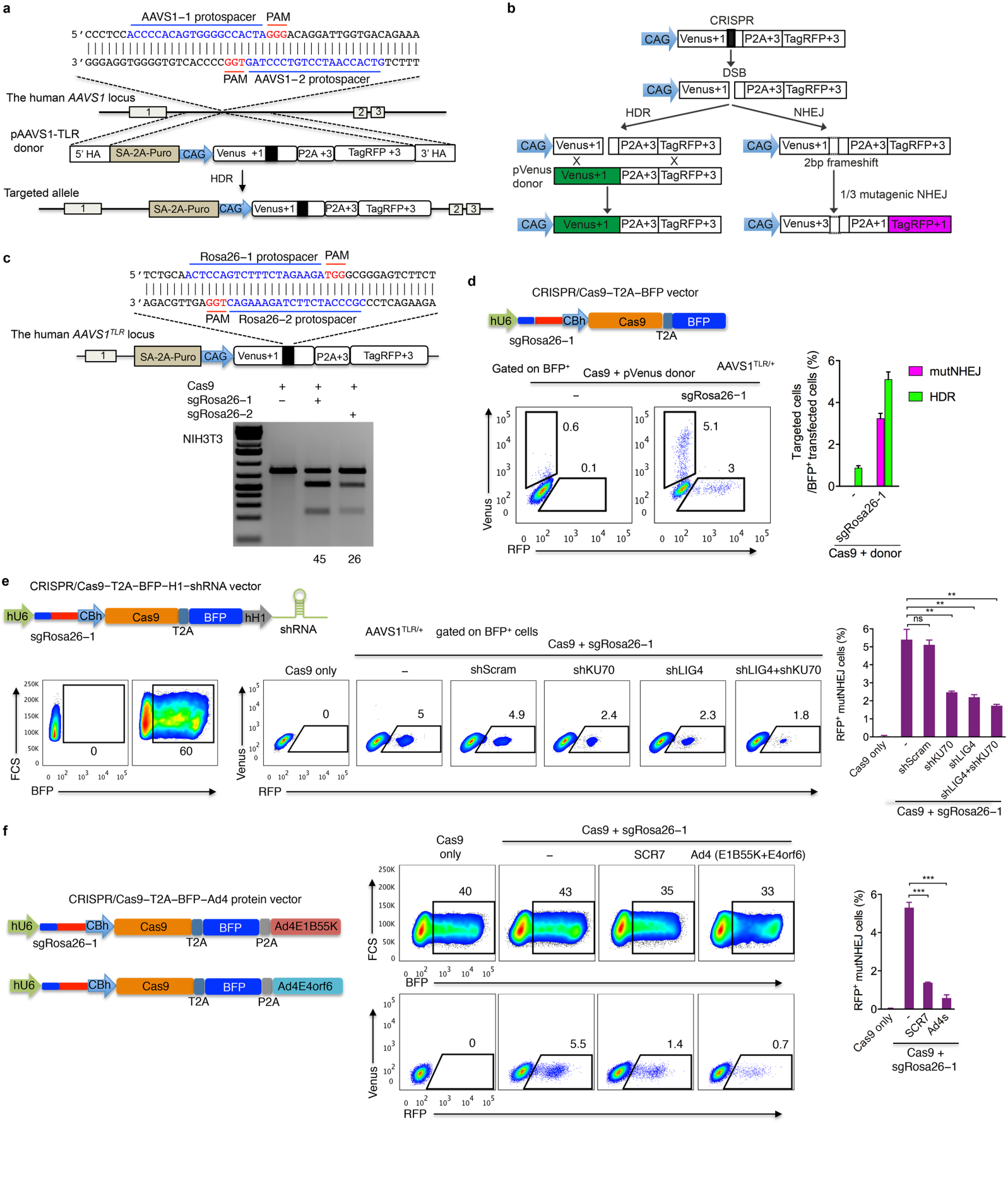
a
AAVS1–1 protospacer
PAM
5′CCCTCCACCCCACAGTGGGGCCACTAGGGACAGGATTGGTGACAGAAA
3′GGGAGGTGGGGTGTCACCCCGGTGATCCCTGTCCTAACCACTGTCTTT
PAM
AAVS1–2 protospacer
The human AAVS1 locus
pAAVS1-TLR donor
5′ HA
SA-2A-Puro
CAG
Venus +1
P2A +3
TagRFP +3
3′ HA
HDR
Targeted allele
b
CRISPR
DSB
HDR
NHEJ
pVenus donor
2bp frameshift
1/3 mutagenic NHEJ
c
Rosa26–1 protospacer
5′TCTGCAACTCCAGTCTTTCTAGAAGATGGGCGGGAGTCTTCT
3′AGACGTTGAGGTCAGAAAGATCTTCTACCCGCCCTCAGAAGA
PAM
Rosa26–2 protospacer
The human AAVS1TLR locus
Cas9
sgRosa26–1
sgRosa26–2
NIH3T3
45
26
d
CRISPR/Cas9–T2A–BFP vector
hU6
CBh
Cas9
BFP
T2A
sgRosa26–1
Gated on BFP+
Cas9 + pVenus donor
AAVS1TLR/+
sgRosa26–1
0.6
0.1
5.1
3
Venus
RFP
Targeted cells /BFP+ transfected cells (%)
mutNHEJ
HDR
Cas9 + donor
e
CRISPR/Cas9–T2A–BFP–H1–shRNA vector
hH1
shRNA
AAVS1TLR/+ gated on BFP+ cells
Cas9 + sgRosa26–1
Cas9 only
shScram
shKU70
shLIG4
shLIG4+shKU70
0
60
5
4.9
2.4
2.3
1.8
FCS
BFP
RFP
RFP+ mutNHEJ cells (%)
ns
f
CRISPR/Cas9–T2A–BFP–Ad4 protein vector
Ad4E1B55K
Ad4E4orf6
P2A
SCR7
Ad4 (E1B55K+E4orf6)
40
43
35
33
0
5.5
1.4
0.7
Ad4s

Figure 2

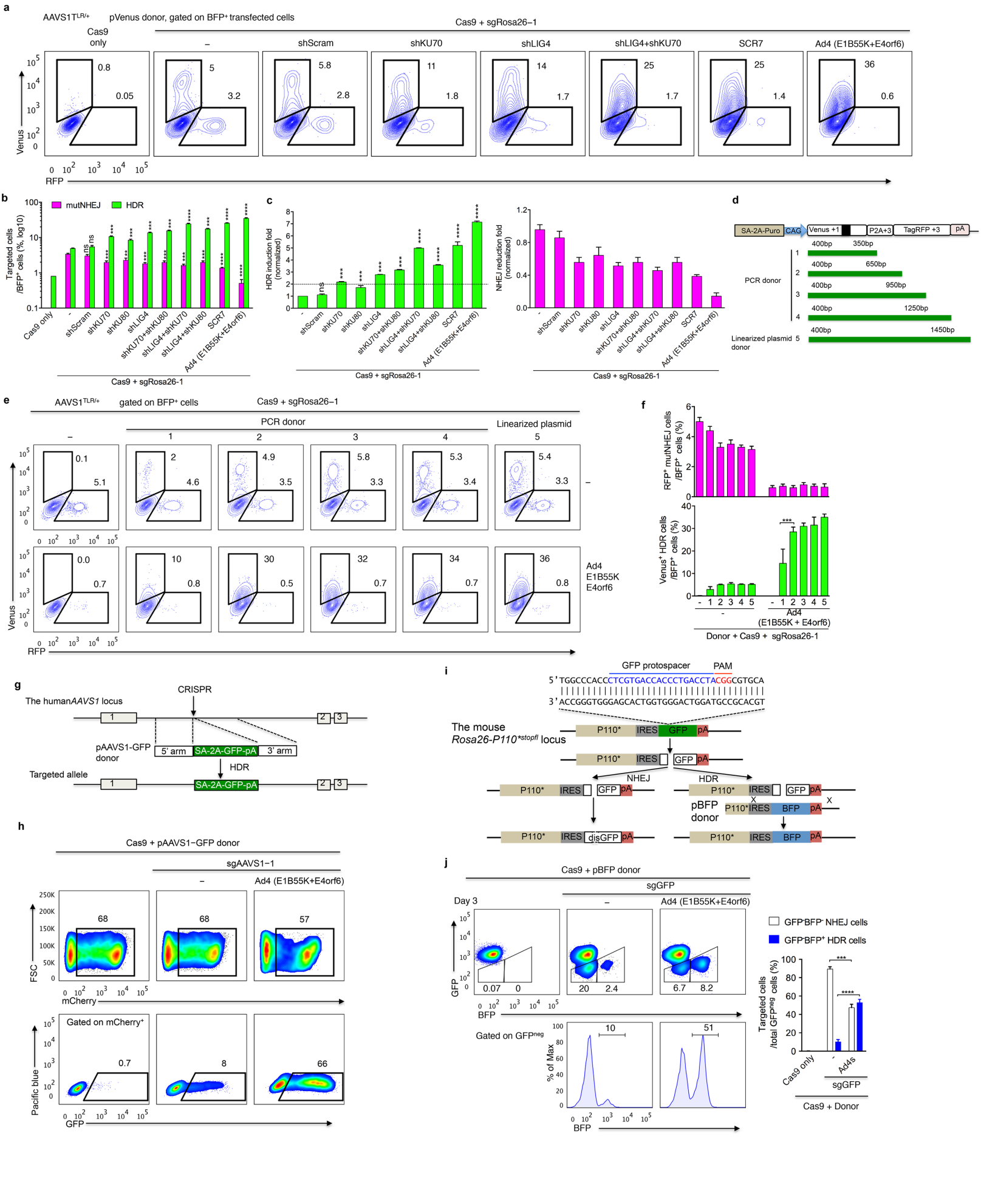
a
AAVS1T^LR/+
pVenus donor, gated on BFP+ transfected cells
Cas9 + sgRosa26–1
Cas9 only
–
shScram
shKU70
shLIG4
shLIG4+shKU70
SCR7
Ad4 (E1B55K+E4orf6)
Venus
RFP
b
mutNHEJ
HDR
Targeted cells /BFP+ cells (%, log10)
Cas9 + sgRosa26-1
c
HDR induction fold (normalized)
NHEJ reduction fold (normalized)
d
SA-2A-Puro
CAG
Venus +1
P2A+3
TagRFP +3
pA
PCR donor
Linearized plasmid donor
400bp
350bp
650bp
950bp
1250bp
1450bp
e
AAVS1^TLR/+
gated on BFP+ cells
PCR donor
Linearized plasmid
Ad4 E1B55K E4orf6
f
RFP+ mutNHEJ cells /BFP+ cells (%)
Venus+ HDR cells /BFP+ cells (%)
Donor + Cas9 + sgRosa26-1
g
The human AAVS1 locus
CRISPR
pAAVS1-GFP donor
5' arm
SA-2A-GFP-pA
3' arm
HDR
Targeted allele
h
Cas9 + pAAVS1–GFP donor
sgAAVS1–1
Gated on mCherry+
i
GFP protospacer
PAM
5'TGGCCCACCCTCGTGACCACCCTGACCTACGGCGTGCA
3'ACCGGGTGGGAGCACTGGTGGGACTGGATGCCGCACGT
The mouse Rosa26-P110*stopfl locus
P110*
IRES
GFP
pA
NHEJ
HDR
pBFP donor
BFP
disGFP
j
Cas9 + pBFP donor
sgGFP
Day 3
Gated on GFPneg
% of Max
GFP-BFP- NHEJ cells
GFP-BFP+ HDR cells
Targeted cells /total GFPneg cells (%)
Cas9 only
Ad4s
Cas9 + Donor

Supplementary Data

Supplementary Fig. 1.1 Strategy for the insertion of the TLR construct into the *AAVS1* locus of HEK293 cells using CRISPR/Cas9.

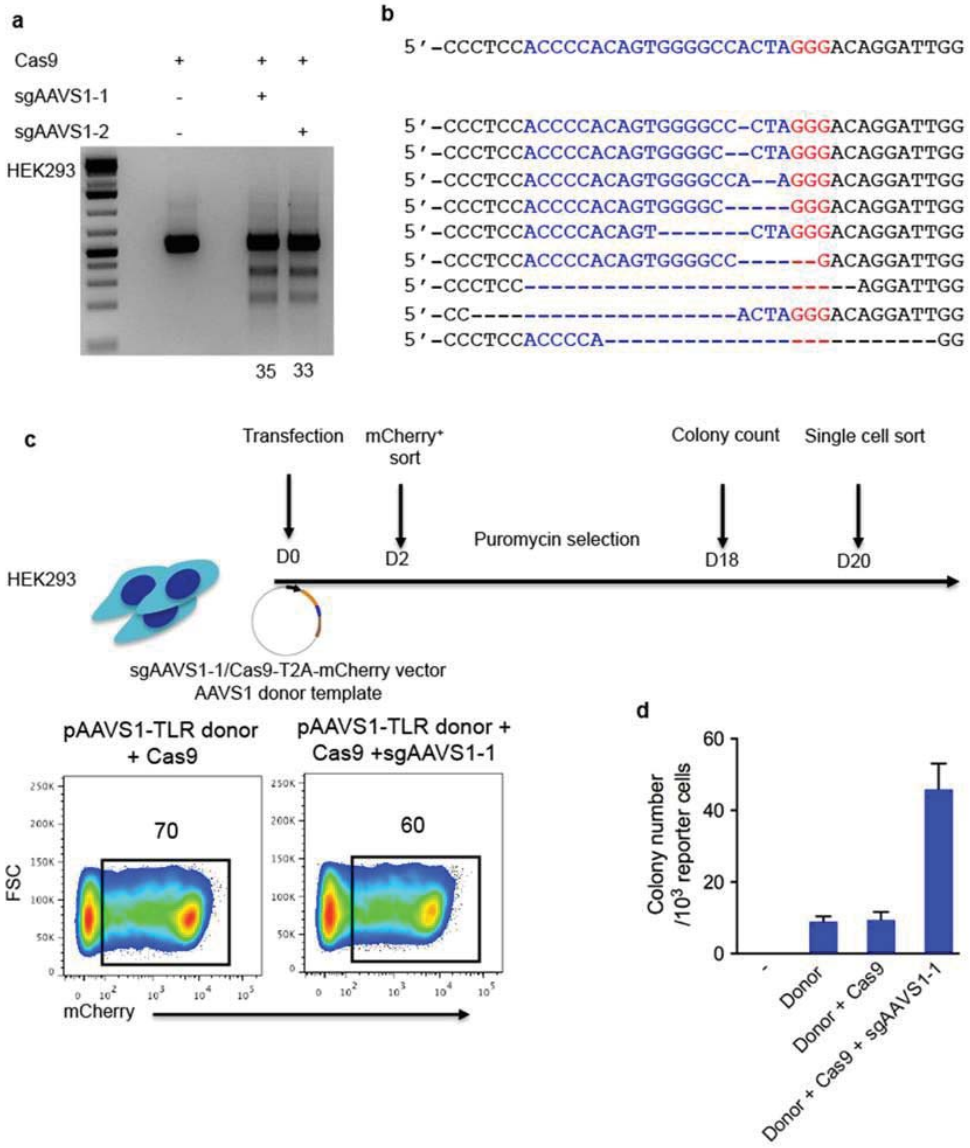

(**a**) T7 endonuclease assay to determine the targeting activity of each sgAAVS1. HEK293 cells were transfected and sorted for Cherry expression at 48h, genomic DNA was extracted and the target region was amplified by PCR. T7EI was added into heteroduplexed PCR products and the reaction products were analyzed by gel electrophoresis and quantified using ImageJ, indicating the cleavage of 35% (sgAAVS1-1) or 33% (sgAAVS1-2) of the PCR products. (**b**) Sequencing of PCR products showed micro-deletions in the targeted AAVS1 locus. (**c**) Scheme of the TLR insertion experiment, HEK293 cells were cotransfected with AAVS1-TLR donor and Cas9-T2A-mCherry or sgAAVS1-1/Cas9-T2A-mCherry expression vectors. mCherry^{+} cells were sorted, selected with puromycin until day 18, the colony number was counted and single cells were sorted. (**d**) The colony number was evaluated for each condition and normalized to the input number of cells.

Supplementary Fig. 1.2 Genotyping PCR for correct integration of the AAVS1-TLR vector into the human *AAVS1* locus.

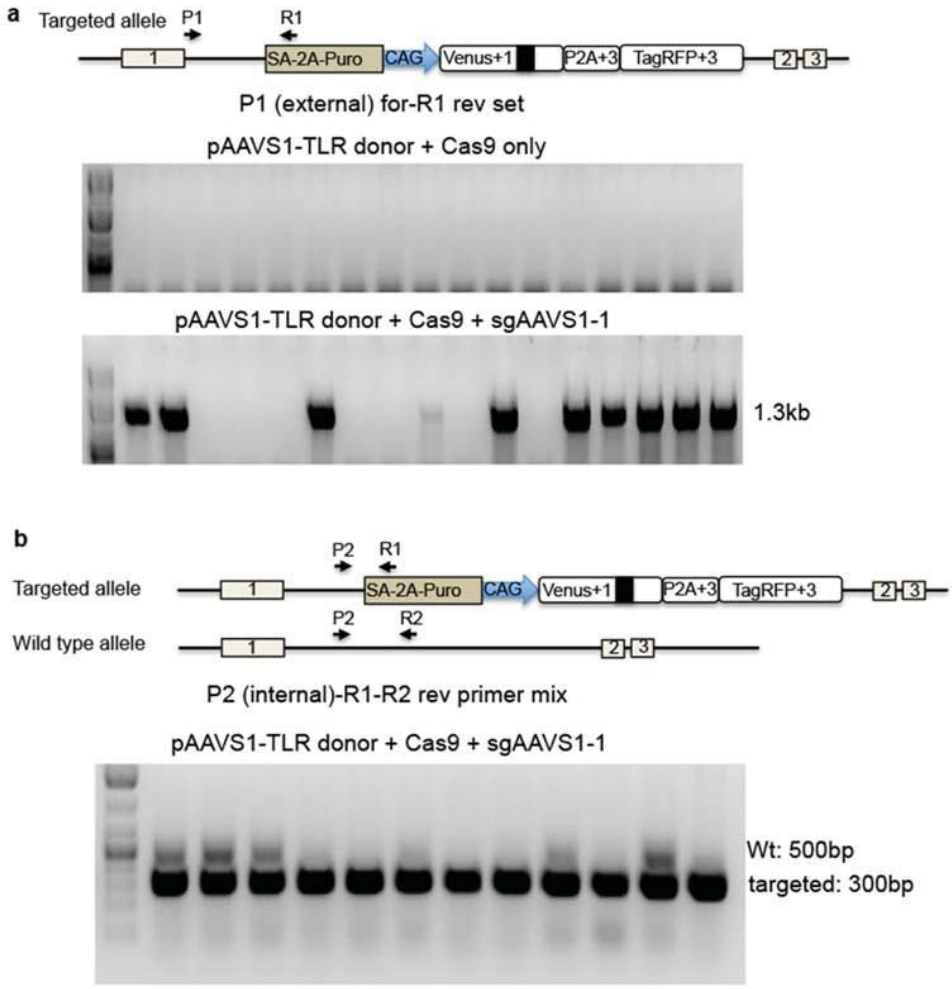

Conditions	Total clones	No of correct integration	Heterozygous/ Homozygous
Donor + Cas9	20	0	0
Donor + Cas9 + sgAAVS1-1	36	21	8/13

(**a**) The human *AAVS1*^{TLR} targeted allele was detected by an external forward primer and a reverse primer located in the inserted cassette. Single cell clones were sorted from cells transfected with pAAVS1-TLR donor and Cas9-expression vector or sgAAVS1-1/Cas9 expression vector. (**b**) Genotyping PCR to detect heterozygous/homozygous clones, the wild type band has a size of ~500 bp and the targeted band is sized ~300 bp.

Supplementary Fig. 1.3 Functional test for the TLR system.

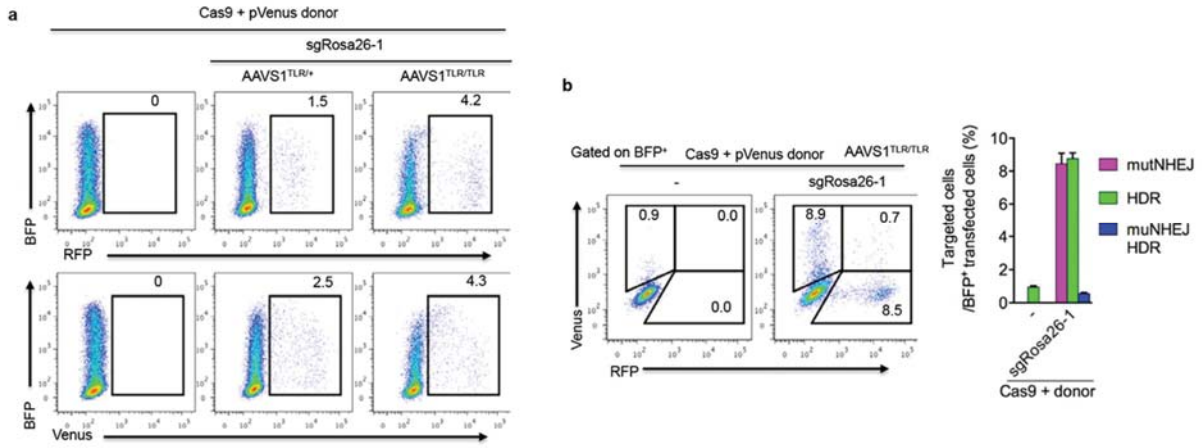

(**a**) Mono- and biallelic AAVS1^{TLR} cells were cotransfected with Venus donor and with Cas9-T2A-BFP expressino vector or with sgRosa26-1/Cas9-T2A-BFP expression vector. The frequency of RFP^{+} mutNHEJ and Venus^{+} HDR cells was analyzed by flow cytometry. (**b**) Gated on BFP^{+} transfected biallelic cells, the fraction of cells undergoing HDR (green column) or NHEJ (red column) or both (blue column) events was further analyzed.

Supplementary Fig. 1.4 Suppression of the NHEJ pathway using shRNA silencing.

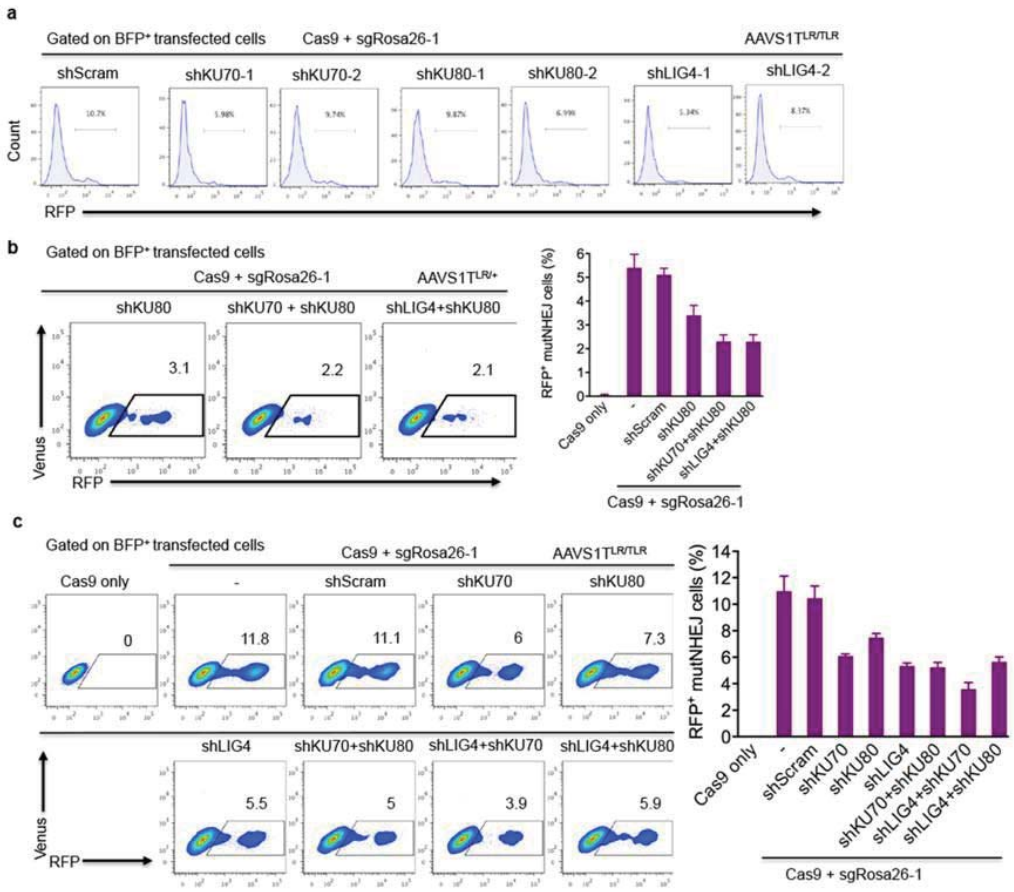

(**a**) For each gene, two shRNAs were selected from published reports and tested for inhibition of NHEJ in biallelic AAVS1$^{TLR/TLR}$ cells (Supplementary Table 4). (**b**) Relates to Fig. 1f, mono-allelic AAVS1$^{TLR/+}$ cells were transfected with CRISPR/Cas9 vector expression shRNA to target KU80 or combinations of KU70, KU80 and Ligase IV. The graph represents triplicate data from 1 of 3 similar experiments. (**c**) Biallelic AAVS1^{TLR} cells were transfected with CRISPR/Cas9 vector expressing shRNA to target KU80 or combinations of KU70, KU80 and DNA Ligase IV. The graphs represent triplicate data from 1 of 3 similar experiments.

Supplementary Fig. 1.5 Suppression of DNA Ligase IV protein by using shRNA or Ad4 proteins.

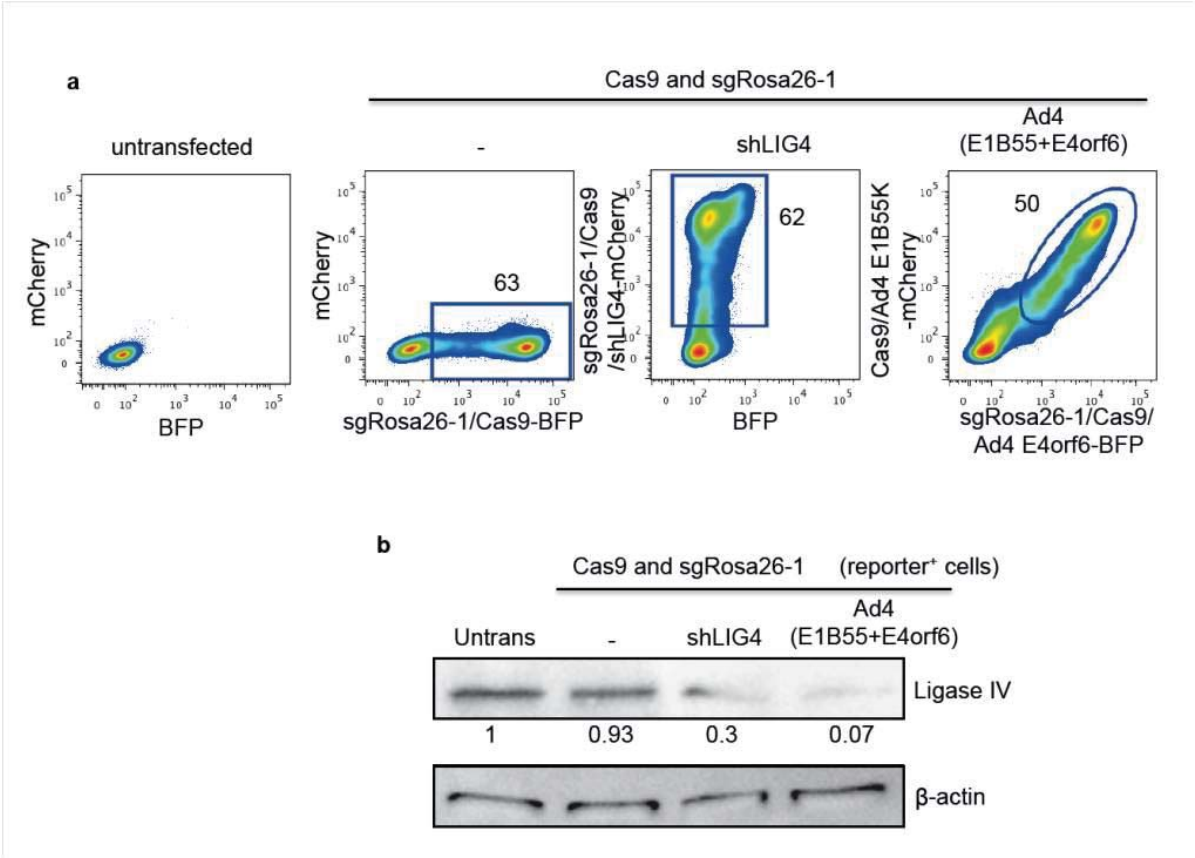

Bi-allelic AAVS1$^{TLR/TLR}$ cells were transfected with sgRosa26-1/Cas9-T2A-BFP, sgRosa26-1/Cas9/shLIG4-T2A-mCherry or co-transfected with sgRosa26-1/Cas9/Ad4 E4orf6-T2A-BFP and Cas9/Ad4 E1B55K-T2A-mCherry expression vectors. (**a**) The transfection efficiency was analysed by flow cytometry at 48h, the reporter^{+} cells sorted. (**b**) Sorted cells were lysed and Western blotting performed for the detection of DNA Ligase IV (103 kDa) and beta-actin (42 kDa). The data represent one of two independent experiments.

Supplementary Fig. 1.6. Inhibition of the NHEJ pathway using the SCR7 inhibitor or overexpression of Ad4 proteins in biallelic AAVS1^{TLR} cells.

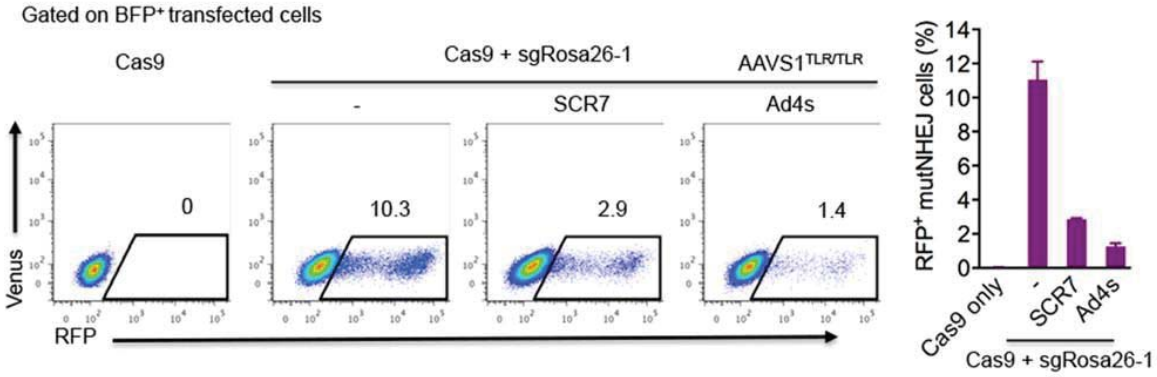

Biallelic AAVS1$^{TLR/TLR}$ cells were transfected with Cas9-T2A-BFP or sgRosa26/Cas9-T2A-BFP expression vectors and treated with SCR7 inhibitor, or were transfected with sgRosa26/Cas9-T2A-BFP-Ad4 E1B55K/ -E4orf6 expression vectors in the absence of SCR7. BFP^{+} transfected cells were analyzed at day 3. The frequency of RFP^{+} mutNHEJ cells is indicated. The data represents 1 of 6 similar experiments.

Supplementary Fig. 2.1 Optimization of HDR efficiency using shRNA silencing.

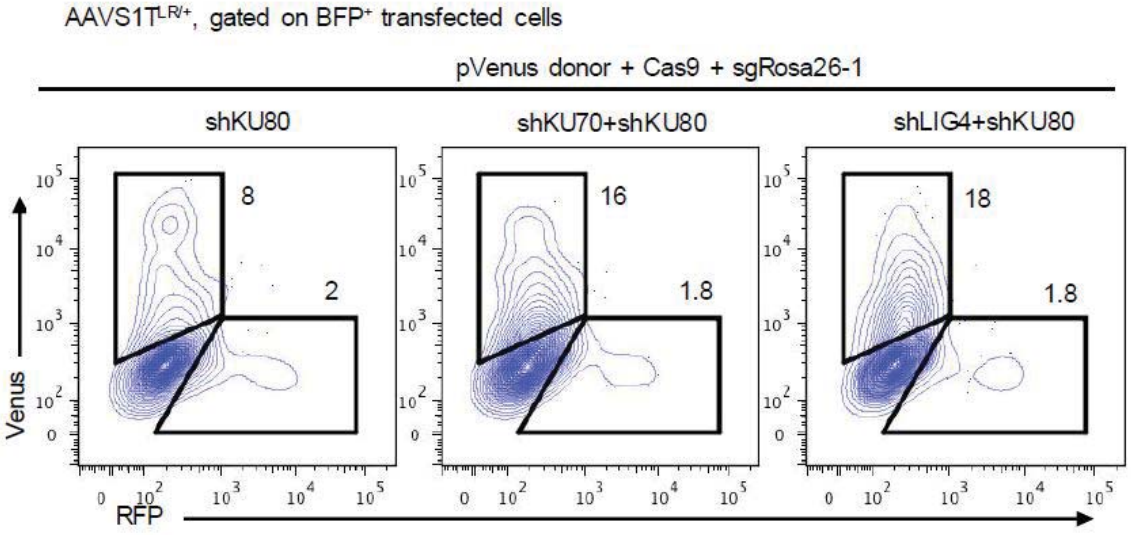

Mono-allelic AAVS1$^{TLR/+}$ cells were transfected with sgRosa26-1, Cas9 and shRNA against KU80 or combinations of KU70 and KU80, or KU80 and DNA Ligase IV. The frequency of Venus^{+} HDR and RFP^{+} mutNHEJ cells, expressed as the percentage of the transfected BFP^{+} cells, was determined at day 3.

Supplementary Fig. 2.2. Suppression of the NHEJ pathway to enhance HDR efficiency for CRISPR/Cas9-mediated gene targeting in biallelic AAVS1$^{TLR/TLR}$ cells.

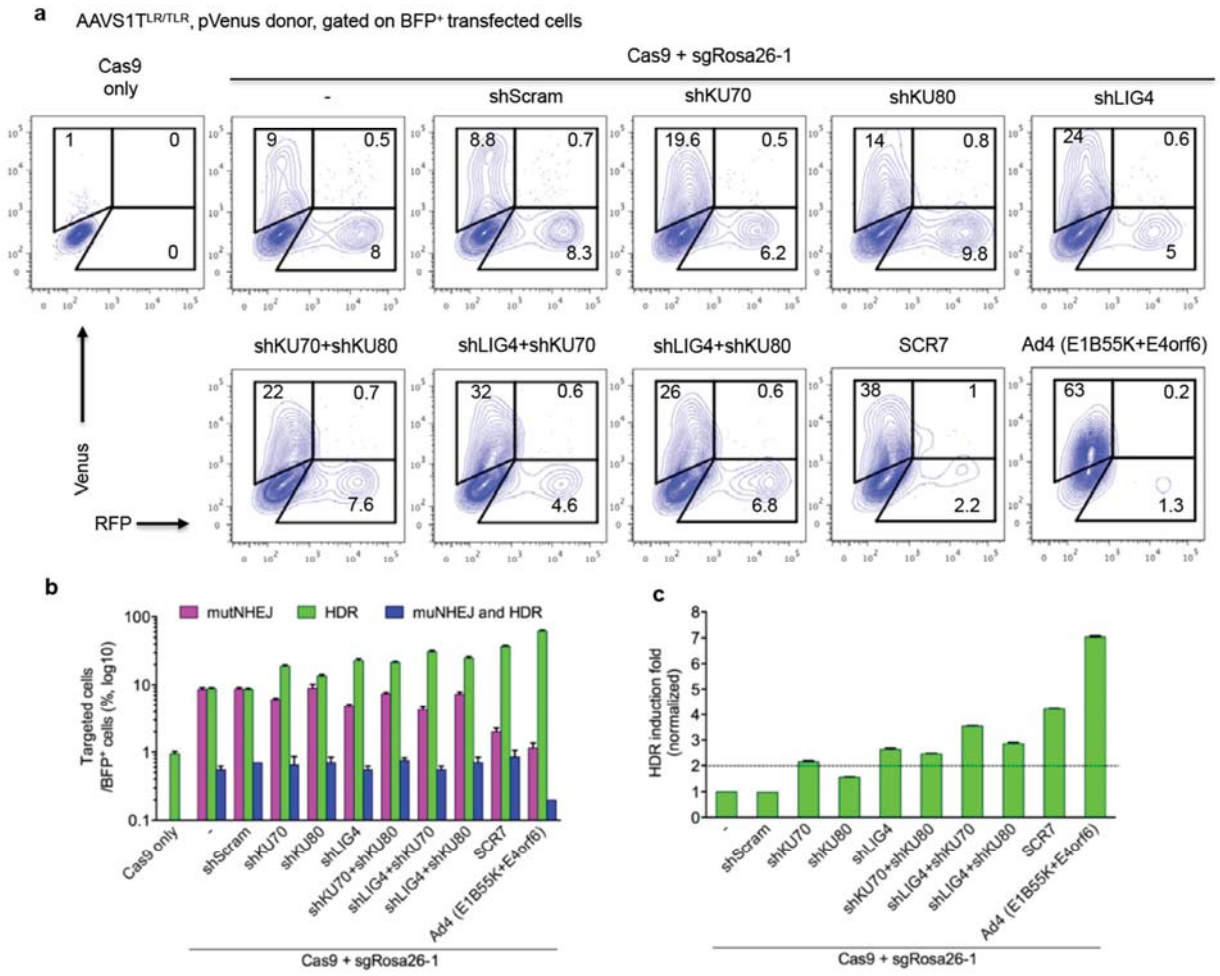

(**a**) Biallelic AAVS1$^{TLR/TLR}$ cells were transfected with Cas9 only or with sgRosa26-1 and Cas9 in the presence of shRNAs for gene silencing or SCR7 inhibitor or the coexpression of Ad4 E1B55K/E4orf6 proteins. The percentage of Venus^{+} HDR (green bars), RFP^{+} mutNHEJ (red bars) and of cells undergoing both events (blue bars) was determined at day 3 by flow cytometry. (**b**) The graph summarizes triplicate data from 1 of 3 similar experiments. (**c**) The normalization of the frequency of Venus^{+} HDR cells to that in cells transfected with sgRosa26-1 and Cas9. The dotted line shows cut of interested fold change.

Supplementary Fig. 2.3. Titration of SCR7 and fluorescence analysis of targeted clones.

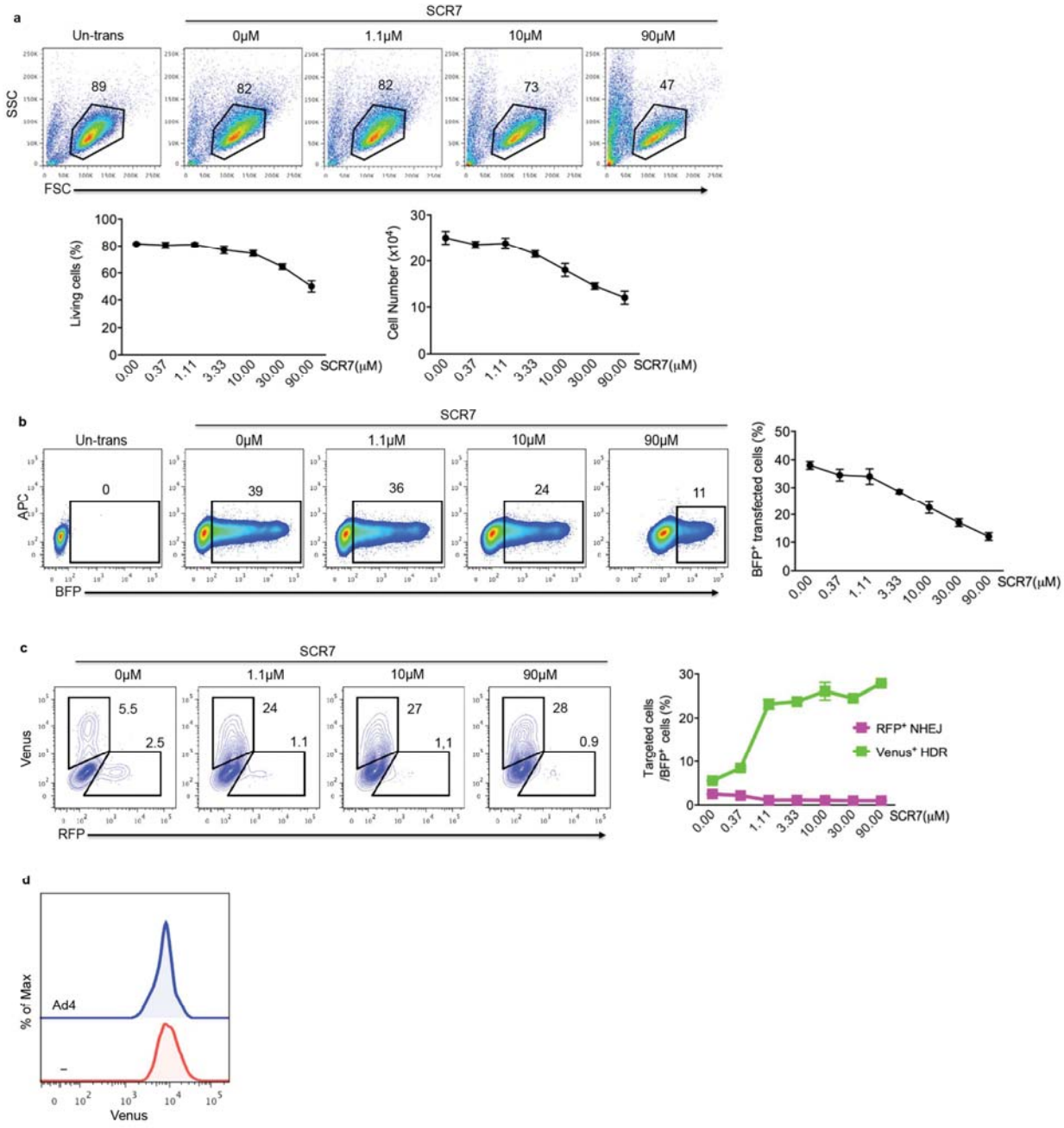

(**a**) AAVS1$^{TLR/+}$ reporter cells were cultured in serial dilutions of SCR7 and analysed at 48h by FACS for the forward (FCS) and side scatter (SSC) parameters. Gating on the population of live cells showed that increasing concentrations of SCR7 lead to a gradual decrease of viability. (**b**) Transfection of

AAVS1$^{TLR/+}$ cells with sgRosa26-1/Cas9-T2A-BFP plasmid and linearized Venus donor vector. The frequency of transfected BFP^{+} cells is reduced in the presence of increasing concentrations of SCR7. (**c**) Gating on transfected BFP^{+} cells, the frequency of Venus^{+} HDR and RFP^{+} mutNHEJ cells was determined at day 3. (**d**) FACS re-analysis of two representative targeted AAVS1$^{TLR/+}$ clones, generated through the coexpression of Ad4 proteins (blue curve) or without Ad4 proteins (red curve) for the expression of Venus signal, showing a similar mean fluorescence intensity, indicating that the reduced reporter expression occurs only transiently.

Supplementary Fig. 2.4. Optimization of PCR donor templates for CRISPR/Cas9-mediated HDR in biallelic AAVS1$^{TLR/TLR}$ cells.

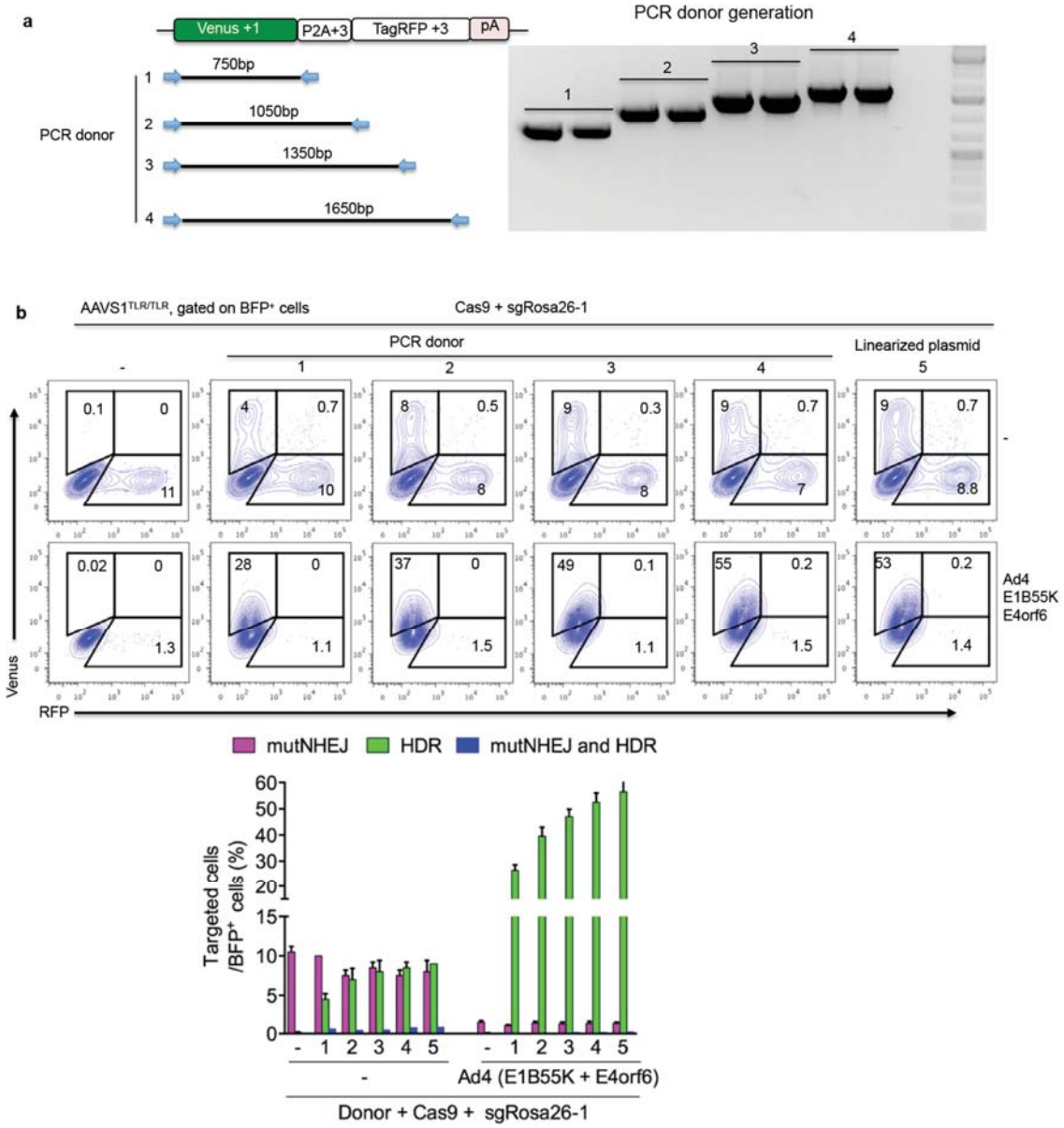

(**a**) Scheme of the forward and reverse primers located in the TLR and the length of PCR donor fragments, the purity of PCR products was shown by agarose gel.(**b**) Biallelic AAVS1$^{TLR/TLR}$ cells were cotransfected with sgRosa26-1/Cas9-T2A-BFP expression vector or coexpression of Ad4 E1B55K/E4orf6 proteins and the same molar concentration of the PCR or linearized Venus plasmid donor. The percentage of Venus$^+$ HDR and RFP$^+$ mutNHEJ cells were analyzed by flow cytometry at 3 days after transfection. The graph summarizes the frequency of RFP$^+$ mutNHEJ (red), Venus$^+$ HDR (green), and RFP$^+$ Venus$^+$ mutNHEJ-HDR (blue) cells. The data represent results from 1 of 2 similar experiments. The bars show mean values ± SD.

Supplementary Fig. 2.5. Detection of correct integration of a GFP cassette into the human *AAVS1* locus.

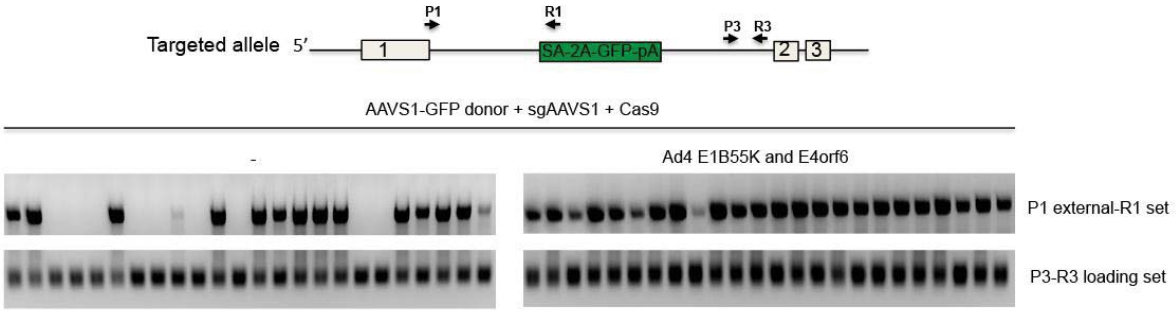

Conditions	No of single cell clones	No of correct integration	% of correct integration
AAVS1-GFP donor+sgAAVS1-1 + Cas9	56	37	66%
AAVS1-GFP donor+sgAAVS1-1 + Cas9 + Ad4 E1B55K and E4orf6	48	45	94%

Scheme of the targeted *AAVS1* allele and primer locations, single cell clones were sorted from HEK293 cells transfected with pAAVS1-GFP donor plasmid and sgAAVS1-1/Cas9-T2A-mCherry or sgAAVS1-1/Cas9-T2A-mCherry-Ad4 E1B55K/E4orf6 expression vectors. PCR was performed using external P1 forward (outside of 5' homology arm) and transgene R1 reverse (seeded in T2A sequence) primers, the PCR products analyzed on agarose gels and the number of correctly integrated clones was calculated. For the genomic DNA loading control, PCR was performed using the P3 forward and R3 reverse primers located outside of the 3' homology arm.

Supplementary Fig. 2.6. CRISPR/Cas9-mediated HDR in mouse Burkitt lymphoma-like cells.

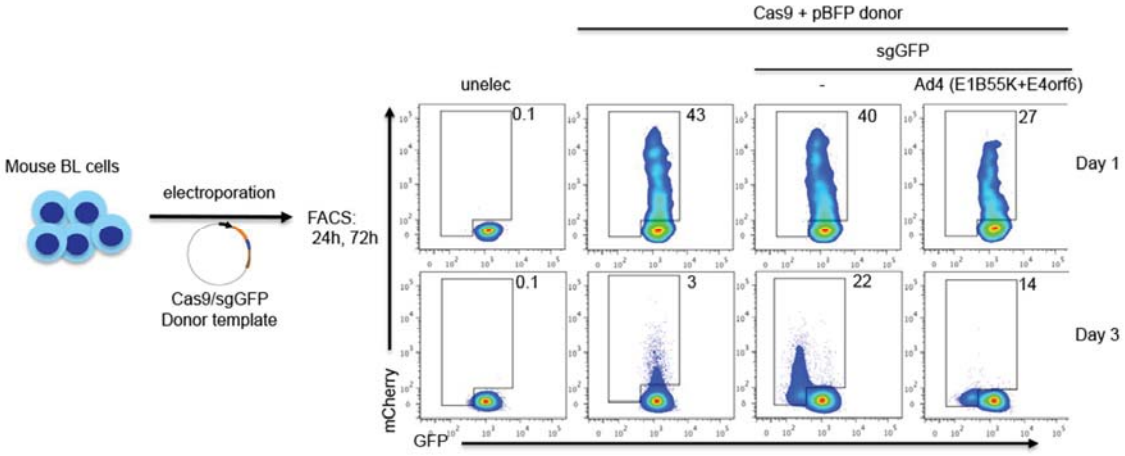

Scheme of CRISPR/Cas9 delivery, mouse BL cells were electroporated to deliver sgGFP/Cas9-T2A-mCherry expression vector or coexpession of Ad4 E1B55K/E4orf6 proteins together with the pBFP donor plasmid. The cells were analysed at 24h or 72h by flow cytometry.

Supplementary Fig. 2.7. Reversion of a *Foxo1* point mutation in mouse Burkitt lymphoma-like cells.

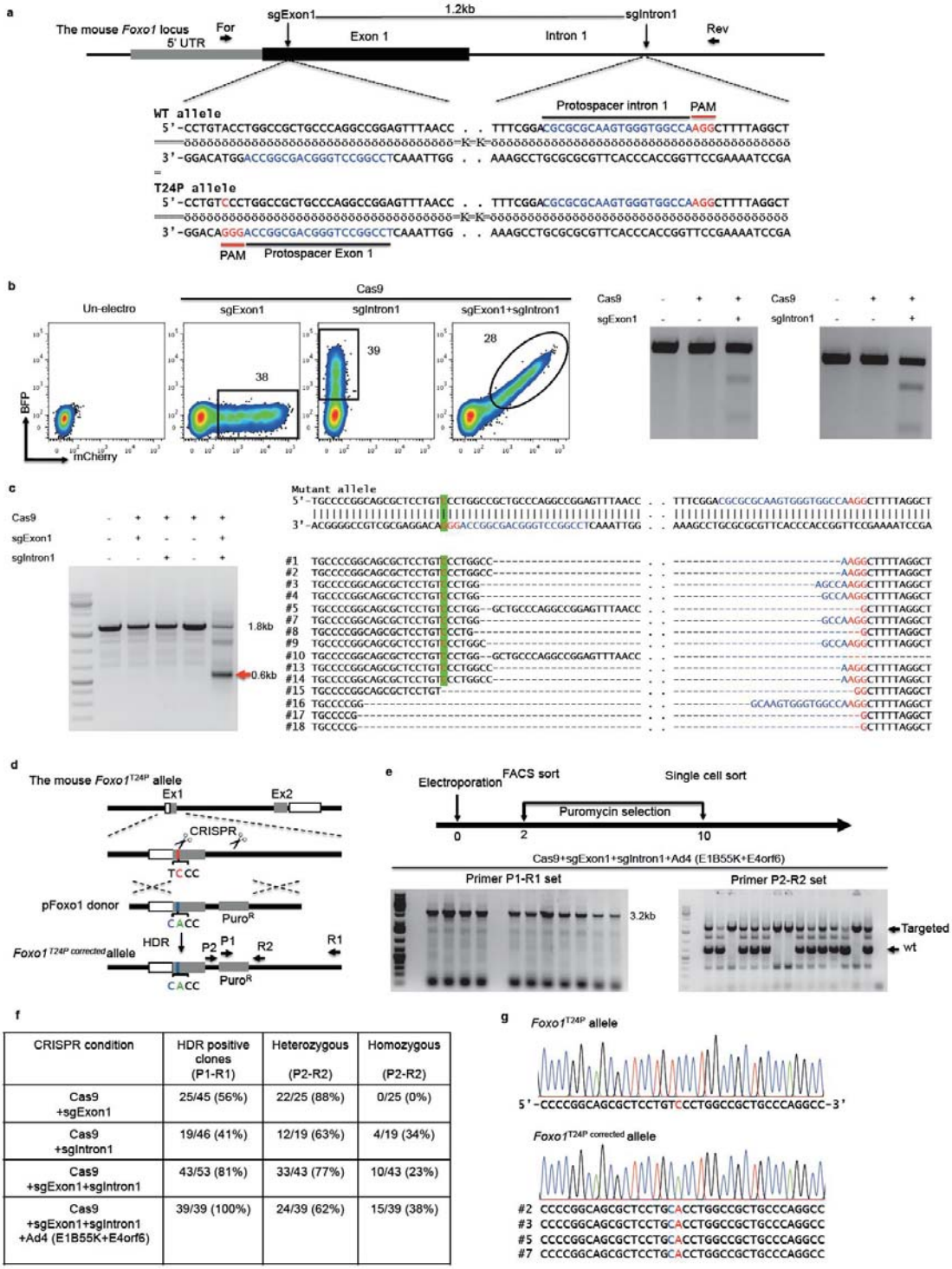

CRISPR condition	HDR positive clones (P1-R1)	Heterozygous (P2-R2)	Homozygous (P2-R2)
Cas9 +sgExon1	25/45 (56%)	22/25 (88%)	0/25 (0%)
Cas9 +sgIntron1	19/46 (41%)	12/19 (63%)	4/19 (34%)
Cas9 +sgExon1+sgIntron1	43/53 (81%)	33/43 (77%)	10/43 (23%)
Cas9 +sgExon1+sgIntron1 +Ad4 (E1B55K+E4orf6)	39/39 (100%)	24/39 (62%)	15/39 (38%)

(**a**) Schematic of the mouse Foxo1 locus, the heterozygous A to C mutation (T24P replacement) in exon 1 generates a PAM (red) sequence which is not present in the wild type allele of Burkitt lymphoma-like (BL) cell line isolated from a tumor bearing mouse. In the targeted sequence, sgRNAs with Foxo1-specific target sequences are indicated in blue and the PAM signal is shown in red. The two sgRNAs are located at a distance of 1.2 kb. (**b**) BL cells were electroporated to deliver sgExon1/Cas9-T2A-mCherry or sgIntron1/Cas9-T2A-BFP plasmid DNA or both expression vectors, as indicated. Reporter positive cells were sorted at 48h, genomic DNA was isolated and a T7EI assay was performed, confirming the activity of both sgRNAs. (**c**) A segment of the Foxo1 locus was PCR amplified using forward and reverse primers as indicated in (a), PCR products derived from undeleted alleles have a size of 1.8 kb whereas the 1.2 kb deletion between the sgRNA target sites leads to a PCR product of 0.6 kb, indicated by a red arrow. PCR products representing the deleted allele were isolated and subcloned into the pSTblue-1 vector for sequencing. Sequence analysis confirmed that the expected 1.2 kb gene segment was deleted in mutant Foxo1 alleles. (**d**) Schematic of codon replacement in the mutant Foxo1 allele of BL cells, the mutant C is highlighted in red, the reverting (wildtype) A is shown in green and an additional silent mutation (T > C) is shown in blue. The pFoxo1 donor vector contains in addition a PGK-Puromycin cassette placed into intron 1. (**e**) Schematic of the codon replacement experiment. Mouse BL cells were co-electroporated with pFoxo1 donor and sgExon1/Cas9-T2A-mCherry or sgIntron1/Cas9-T2A-BFP plasmids or with both expression vectors in the presence or absence of the Ad4 proteins. Reporter positive cells were sorted on day 2 and selected with Puromycin for 8 days. At day 10 single cells were sorted, expanded into clones and genomic DNA was isolated. The mouse Foxo1 targeted allele was detected by PCR amplification of a 3.2 kb fragment using an external reverse primer and a forward primer located in the Puromycin cassette (P1-R1 set). The genotyping PCR to distinguish heterozygous and homozygous targeted clones was performed with the P2-R2 primer pair, detecting the wildtype allele by a 700 bp band and targeted loci by a 2 kb band. (**f**) Summary of the frequency of Foxo1 targeted clones and of heterozygous and homozygous targeting events using the indicated transfection conditions. (**g**) Sequencing of PCR products derived from targeted clones confirmed that the mutant *Foxo1* allele was successfully repaired.

Supplementary Table 1 Gene and protein sequences used this study.

Gene name	Sequence (5' to 3')
The TLR DNA sequence Venus – green Rosa26 sequence – pink, Rab38 sequence – brown, venus - green (tag: stop), MluI site - black Underlined(tg: 2 bp frameshift) T2A – black TagRFP – red (tga: stop)	ATGGTGAGCAAGGGCGAGGAGCTGTTCACCGGGGTGGTGCCCATCCTGGTCGAGCTGGACGGCGACGTAAACGG CCACAAGTTCAGCGTGTCCGGCGAGGGCGAGGGCGATGCCACCTACGGCAAGCTGACCCTGAAGCTGATCTGCA CCACCGGCAAGCTGCCCGTGCCCTGGCCCACCCTCGTGACCACCCTGGGCTACGGCCTGCAGTGCTTCGCCCGC TACCCCGACCACATGAAGCAGCACGACTTCTTCAAGTCCGCCATGCCCGAAGGCTACGTCCAGGAGCGCACCAT CTTCTTCAAGGACGACGGCAACTACAAGACCCGCGCCGAGGTGAAGTTCGAGCTGCAACTCCAGTCTTTCTAGA AGATGGGCGGGAGTCTTCTGGGCAGGCTTATATCAAGCGCTATGTGCACCAAAACTTCTCCTCGCACTACCGGG CCACCATTGGTGATCACCGCCGACAAGCAGAAGAACGGCATCAAGGCCAACTTCAAGATCCGCCACAACATCGA GGACGGCGGCGTGCAGCTCGCCGACCACTACCAGCAGAACACCCCCATCGGCGACGGCCCCGTGCTGCTGCCCG ACAACCACTACCTGAGCTACCAGTCCGCCCTGAGCAAAGACCCCAACGAGAAGCGCGATCACATGGTCCTGCTG GAGTTCGTGACCGCCGCCGGGATCACTCTCGGCATGGACGAGCTGTACAAGtag**ACGCGTtgGCCACGAACTTC** **TCTCTGTTAAAGCAAGCAGGAGATGTTGAAGAAAACCCCGGGCCT**ATGGTGTCTAAGGGCGAAGAGCTGATTAA GGAGAACATGCACATGAAGCTGTACATGGAGGGCACCGTGAACAACCACCACTTCAAGTGCACATCCGAGGGCG AAGGCAAGCCCTACGAGGGCACCCAGACCATGAGAATCAAGGTGGTCGAGGGCGGCCCTCTCCCCTTCGCCTTC GACATCCTGGCTACCAGCTTCATGTACGGCAGCAGAACCTTCATCAACCACACCCAGGGCATCCCCGACTTCTT TAAGCAGTCCTTCCCTGAGGGCTTCACATGGGAGAGAGTCACCACATACGAAGACGGGGGCGTGCTGACCGCTA CCCAGGACACCAGCCTCCAGGACGGCTGCCTCATCTACAACGTCAAGATCAGAGGGGTGAACTTCCCATCCAAC GGCCCTGTGATGCAGAAGAAAACACTCGGCTGGGAGGCCAACACCGAGATGCTGTACCCCGCTGACGGCGGCCT GGAAGGCAGAAGCGACATGGCCCTGAAGCTCGTGGGCGGGGGCCACCTGATCTGCAACTTCAAGACCACATACA GATCCAAGAAACCCGCTAAGAACCTCAAGATGCCCGGCGTCTACTATGTGGACCACAGACTGGAAAGAATCAAG GAGGCCGACAAAGAGACCTACGTCGAGCAGCACGAGGTGGCTGTGGCCAGATACTGCGACCTCCCTAGCAAACT GGGGCACAAACTTAATtga
Adenovirus 4 (NCBI accession No. NC_003266) **E4ORF6 protein**	MSGNSSIMTRSRTRLALSRHHPYQPPATLPRCEETESRASLVEDHPVLPDCDTLSMHNVSSVRGLP CSAGFTVLQEFPVPWDMVLTPEELRVLKTCMSVCLCCANIDLFSSQLIHGRERWVIHCHCQNPGSL RCMAGGTVLAIWFRRIIQGCMFNQRVMWYREVVNLHMPKEIMYMGSVFWRGRHLIYIRIWYDGHV GSIVPQMSFGWSTLNYGLLNNLVVLCCTYCSDLSEIRIRCCARRTRRLMLRAIGIMRRESLDPDPLS SSLTERRRQRLLRGLMRHNRPIPFADYDSHRSYSR*
Adenovirus 4 **E1B55K protein**	MESRNPFQQGLPAGFLSSSFVENMEVPAPECNLRLLAGTAARHSEDPESPAAGGSRRE SESRPGPSGGGVADLFPELHRVLTRSSSGRERGIKRERHDETNHRIELTVGLMSRKRPE TVWWYEVQSTGTDEVSVMHERFSLEQVKTCWLEPEDDWEVAIRNYAKLALRPDRKYKI TKLINIRNACYISGNGAEVEICLQDRVAFRCCMMNMYPGVVDMDGVTFMNMRFRGDGY NGTVFMANTKLTVHGCSFFGFNNTCIEAWGQVGVKGCSFSANWMGVVGRTKSMLSVK KCLFERCHLGVMSEGEARIRHCASTETGCFVLCKGNAKIKHNMICGASDERGYQMLTCA GGNSHMLAAVHVASHSRKPWPEFEHNVMTRCNMHLGARRGMFMPYQCNLNYVKVLLE PDVMSRVSLTGVFDMNVEVWKILRYDEYKTRCRACECGGKHARFQPVCVDVTEDLRPD HLVLSCTGTEFGSSGEESD*

Supplementary Table 2 Sequencing of the traffic light reporter in 10 individual clones after HDR-mediated repair of the Venus gene.

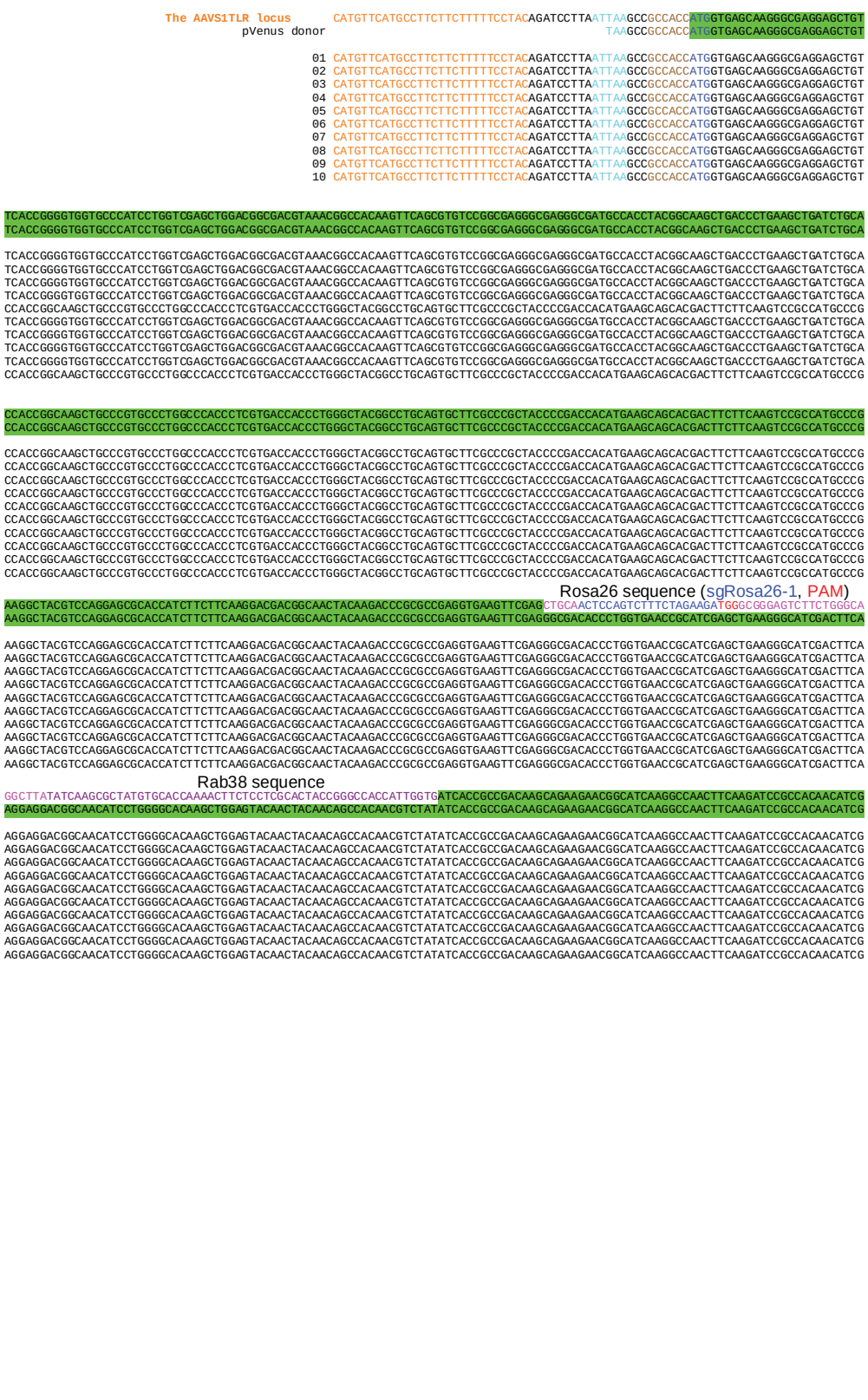

Supplementary Table 3 Sequencing data confirms the SA-T2A-GFP insertion into the human *AAVS1* locus.

Sequences in the junctions of the 5' homology arm (Targeting without adenoviral proteins)

```
                 outside of homology arm                          inside of homology arm
   ACTGGCTTCTGCGCCGCCTCTGGCCCACTGTTTCCCCTTCCCAGGCAGGTCCTGCTTTCTCTGACCTGCATTCTCTCCCCTGGGCCTGTGCCGCTTTCTG[...]

01 ACTGGCTTCTGCGCCGCCTCTGGCCCACTGTTTCCCCTTCCCAGGCAGGTCCTGCTTTCTCTGACCAGCATTCTCTCCCCTGGGCCTGTGCCGCTTTCTG[...]
02 ACTGGCTTCTGCGCCGCCTCTGGCCCACTGTTTCCCCTTCCCAGGCAGGTCCTGCTTTCTCTGACCTGCATTCTCTCCCCTGGGCCTGTGCCGCTTTCTG[...]
03 ACTGGCTTCTGCGCCGCCTCTGGCCCACTGTTTCCCCTTCCCAGGCAGGTCCTGCTTTCTCTGACCTGCATTCTCTCCCCTGGGCCTGTGCCGCTTTCTG[...]
04 ACTGGCTTCTGCGCCGCCTCTGGCCCACTGTTTCCCCTTCCCAGGCAGGTCCTGCTTTCTCTGACCTGCATTCTCTCCCCTGGGCCTGTGCCGCTTTCTG[...]
05 ACTGGCTTCTGCGCCGCCTCTGGCCCACTGTTTCCCCTTCCCAGGCAGGTCCTGCTTTCTCTGACCTGCATTCTCTCCCCTGGGCCTGTGCCGCTTTCTG[...]
06 ACTGGCTTCTGCGCCGCCTCTGGCCCACTGTTTCCCCTTCCCAGGCAGGTCCTGCTTTCTCTGACCTGCATTCTCTCCCCTGGGCCTGTGCCGCTTTCTG[...]
07 ACTGGCTTCTGCGCCGCCTCTGGCCCACTGTTTCCCCTTCCCAGGCAGGTCCTGCTTTCTCTGACCTGCATTCTCTCCCCTGGGCCTGTGCCGCTTTCTG[...]
08 ACTGGCTTCTGCGCCGCCTCTGGCCCACTGTTTCCCCTTCCCAGGCAGGTCCTGCTTTCTCTGACCTGCATTCTCTCCCCTGGGCCTGTGCCGCTTTCTG[...]
10 ACTGGCTTCTGCGCCGCCTCTGGCCCACTGTTTCCCCTTCCCAGGCAGGTCCTGCTTTCTCTGACCTGCATTCTCTCCCCTGGGCCTGTGCCGCTTTCTG[...]
11 ACTGGCTTCTGCGCCGCCTCTGGCCCACTGTTTCCCCTTCCCAGGCAGGTCCTGCTTTCTCTGACCTGCATTCTCTCCCCTGGGCCTGTGCCGCTTTCTG[...]
12 ACTGGCTTCTGCGCCGCCTCTGGCCCACTGTTTCCCCTTCCCAGGCAGGTCCTGCTTTCTCTGACCTGCATTCTCTCCCCTGGGCCTGTGCCGCTTTCTG[...]

                   inside of homology arm                               SA-T2A sequence
   [...]GGCTCTGGTTCTGGGTACTTTTATCTGTCCCCTCCACCCCACAGTGGGGCAAGCTTCTGACCTCTTCTCTTCCTCCCACAGGGCCTCGAGAGATCTGGCA

   [...]GGCTCTGGTTCTGGGTACTTTTATCTGTCCCCTCCACCCCACAGTGGGGCAAGCTTCTGACCTCTTCTCTTCCTCCCACAGGGCCTCGAGAGATCTGGCA
   [...]GGCTCTGGTTCTGGGTACTTTTATCTGTCCCCTCCACCCCACAGTGGGGCAAGCTTCTGACCTCTTCTCTTCCTCCCACAGGGCCTCGAGAGATCTGGCA
   [...]GGCTCTGGTTCTGGGTACTTTTATCTGTCCCCTCCACCCCACGGTGGGGCAAGCTTCTGACCTCTTCTCTTCCTCCCACAGGGCCTCGAGAGATCTGGCA
   [...]GGCTCTGGTTCTGGGTACTTTTATCTGTCCCCTCCACCCCACAGTGGGGCAAGCTTCTGACCTCTTCTCTTCCTCCCACAGGGCCTCGAGAGATCTGGCA
   [...]GGCTCTGGTTCTGGGTACTTTTATCTGTCCCCTCCACCCCACAGTGGGGCAAGCTTCTGACCTCTTCTCTTCCTCCCACAGGGCCTCGAGAGATCTGGCA
   [...]GGCTCTGGTTCTGGGTACTTTTATCTGTCCCCTCCACCCCACAGTGGGGCAAGCTTCTGACCTCTTCTCTTCCTCCCACAGGGCCTCGAGAGATCTGGCA
   [...]GGCTCTGGTTCTGGGTACTTTTATCTGTCCCCTCCACCCCACAGTGGGGCAAGCTTCTGACCTCTTCTCTTCCTCCCACAGGGCCTCGAGAGATCTGGCA
   [...]GGCTCTGGTTCTGGGTACTTTTATCTGTCCCCTCCACCCCACAGTGGGGCAAGCTTCTGACCTCTTCTCTTCCTCCCACAGGGCCTCGAGAGATCTGGCA
   [...]GGCTCTGGTTCTGGGTACTTTTATCTGTCCCCTCCACCCCACAGTGGGGCAAGCTTCTGACCTCTTCTCTTCCTCCCACAGGGCCTCGAGAGATCTGGCA
   [...]GGCTCTGGTTCTGGGTACTTTTATCTGTCCCCTCCACCCCACAGTGGGGCAAGCTTCTGACCTCTTCTCTTCCTCCCACAGGGCCTCGAGAGATCTGGCA
   [...]GGCTCTGGTTCTGGGTACTTTTATCTGTCCCCTCCACCCCACAGTGGGGCAAGCTTCTGACCTCTTCTCTTCCTCCCACAGGGCCTCGAGAGATCTGGCA
   [...]GGCTCTGGTTCTGGGTACTTTTATCTGTCCCCTCCACCCCACAGTGGGGCAAGCTTCTGACCTCTTCTCTTCCTCCCACAGGGCCTCGAGAGATCTGGCA
```

Sequences in the junctions of the 5' homology arm (Targeting with adenoviral proteins)

```
                 outside of homology arm                          inside of homology arm
   ACTGGCTTCTGCGCCGCCTCTGGCCCACTGTTTCCCCTTCCCAGGCAGGTCCTGCTTTCTCTGACCTGCATTCTCTCCCCTGGGCCTGTGCCGCTTTCTG[...]

01 ACTGGCTTCTGCGCCGCCTCTGGCCCACTGTTTCCCCTTCCCAGGCAGGTCCTGCTTTCTCTGACCAGCATTCTCTCCCCTGGGCCTGTGCCGCTTTCTG[...]
02 ACTGGCTTCTGCGCCGCCTCTGGCCCACTGTTTCCCCTTCCCAGGCAGGTCCTGCTTTCTCTGACCTGCATTCTCTCCCCTGGGCCTGTGCCGCTTTCTG[...]
03 ACTGGCTTCTGCGCCGCCTCTGGCCCACTGTTTCCCCTTCCCAGGCAGGTCCTGCTTTCTCTGACCTGCATTCTCTCCCCTGGGCCTGTGCCGCTTTCTG[...]
04 ACTGGCTTCTGCGCCGCCTCTGGCCCACTGTTTCCCCTTCCCAGGCAGGTCCTGCTTTCTCTGACCTGCATTCTCTCCCCTGGGCCTGTGCCGCTTTCTG[...]
05 ACTGGCTTCTGCGCCGCCTCTGGCCCACTGTTTCCCCTTCCCAGGCAGGTCCTGCTTTCTCTGACCTGCATTCTCTCCCCTGGGCCTGTGCCGCTTTCTG[...]
06 ACTGGCTTCTGCGCCGCCTCTGGCCCACTGTTTCCCCTTCCCAGGCAGGTCCTGCTTTCTCTGACCTGCATTCTCTCCCCTGGGCCTGTGCCGCTTTCTG[...]
07 ACTGGCTTCTGCGCCGCCTCTGGCCCACTGTTTCCCCTTCCCAGGCAGGTCCTGCTTTCTCTGACCTGCATTCTCTCCCCTGGGCCTGTGCCGCTTTCTG[...]
08 ACTGGCTTCTGCGCCGCCTCTGGCCCACTGTTTCCCCTTCCCAGGCAGGTCCTGCTTTCTCTGACCTGCATTCTCTCCCCTGGGCCTGTGCCGCTTTCTG[...]
10 ACTGGCTTCTGCGCCGCCTCTGGCCCACTGTTTCCCCTTCCCAGGCAGGTCCTGCTTTCTCTGACCTGCATTCTCTCCCCTGGGCCTGTGCCGCTTTCTG[...]
11 ACTGGCTTCTGCGCCGCCTCTGGCCCACTGTTTCCCCTTCCCAGGCAGGTCCTGCTTTCTCTGACCTGCATTCTCTCCCCTGGGCCTGTGCCGCTTTCTG[...]
12 ACTGGCTTCTGCGCCGCCTCTGGCCCACTGTTTCCCCTTCCCAGGCAGGTCCTGCTTTCTCTGACCTGCATTCTCTCCCCTGGGCCTGTGCCGCTTTCTG[...]
13 ACTGGCTTCTGCGCCGCCTCTGGCCCACTGTTTCCCCTTCCCAGGCAGGTCCTGCTTTCTCTGACCTGCATTCTCTCCCCTGGGCCTGTGCCGCTTTCTG[...]

                   inside of homology arm                               SA-T2A sequence
   [...]GGCTCTGGTTCTGGGTACTTTTATCTGTCCCCTCCACCCCACAGTGGGGCAAGCTTCTGACCTCTTCTCTTCCTCCCACAGGGCCTCGAGAGATCTGGCA

   [...]GGCTCTGGTTCTGGGTACTTTTATCTGTCCCCTCCACCCCACAGTGGGGCAAGCTTCTGACCTCTTCTCTTCCTCCCACAGGGCCTCGAGAGATCTGGCA
   [...]GGCTCTGGTTCTGGGTACTTTTATCTGTCCCCTCCACCCCACAGTGGGGCAAGCTTCTGACCTCTTCTCTTCCTCCCACAGGGCCTCGAGAGATCTGGCA
   [...]GGCTCTGGTTCTGGGTACTTTTATCTGTCCCCTCCACCCCACGGTGGGGCAAGCTTCTGACCTCTTCTCTTCCTCCCACAGGGCCTCGAGAGATCTGGCA
   [...]GGCTCTGGTTCTGGGTACTTTTATCTGTCCCCTCCACCCCACAGTGGGGCAAGCTTCTGACCTCTTCTCTTCCTCCCACAGGGCCTCGAGAGATCTGGCA
   [...]GGCTCTGGTTCTGGGTACTTTTATCTGTCCCCTCCACCCCACAGTGGGGCAAGCTTCTGACCTCTTCTCTTCCTCCCACAGGGCCTCGAGAGATCTGGCA
   [...]GGCTCTGGTTCTGGGTACTTTTATCTGTCCCCTCCACCCCACAGTGGGGCAAGCTTCTGACCTCTTCTCTTCCTCCCACAGGGCCTCGAGAGATCTGGCA
   [...]GGCTCTGGTTCTGGGTACTTTTATCTGTCCCCTCCACCCCACAGTGGGGCAAGCTTCTGACCTCTTCTCTTCCTCCCACAGGGCCTCGAGAGATCTGGCA
   [...]GGCTCTGGTTCTGGGTACTTTTATCTGTCCCCTCCACCCCACAGTGGGGCAAGCTTCTGACCTCTTCTCTTCCTCCCACAGGGCCTCGAGAGATCTGGCA
   [...]GGCTCTGGTTCTGGGTACTTTTATCTGTCCCCTCCACCCCACAGTGGGGCAAGCTTCTGACCTCTTCTCTTCCTCCCACAGGGCCTCGAGAGATCTGGCA
   [...]GGCTCTGGTTCTGGGTACTTTTATCTGTCCCCTCCACCCCACAGTGGGGCAAGCTTCTGACCTCTTCTCTTCCTCCCACAGGGCCTCGAGAGATCTGGCA
   [...]GGCTCTGGTTCTGGGTACTTTTATCTGTCCCCTCCACCCCACAGTGGGGCAAGCTTCTGACCTCTTCTCTTCCTCCCACAGGGCCTCGAGAGATCTGGCA
   [...]GGCTCTGGTTCTGGGTACTTTTATCTGTCCCCTCCACCCCACAGTGGGGCAAGCTTCTGACCTCTTCTCTTCCTCCCACAGGGCCTCGAGAGATCTGGCA
```

Supplementary Table 4 Oligonucleotides used in this study

Oligonucleotides used for cloning of sgRNA expression vectors		
Gene target	Direction	Sequence (5' to 3')
Human *AAVS1-1*	F	CACCGACCCCACAGTGGGGCCACTA
	R	AAACTAGTGGCCCCACTGTGGGGTC
Human *AAVS1-2*	F	CACCGTCACCAATCCTGTCCCTAG
	R	AAACCTAGGGACAGGATTGGTGAC
Mouse *Rosa26-1*	F	CACCGACTCCAGTCTTTCTAGAAGA
	R	AAACTCTTCTAGAAAGACTGGAGTC
Mouse *Rosa26-2*	F	CACCGCGCCCATCTTCTAGAAAGAC
	R	AAACGTCTTTCTAGAAGATGGGCGC
GFP reporter gene	F	CACCGCTCGTGACCACCCTGACCTA
	R	AAACTAGGTCAGGGTGGTCACGAGC

Oligonucleotides used for cloning of shRNA expression vectors The shRNAs to target NHEJ molecules were selected from previous reports (see references) and cloned into the BamHI/AflII sites of the CRISPR/Cas9-T2A-BFP-hH1 vector.	
Gene target	Target sequence (5' to 3')
KU70-1	GGAAGAGATAGTTTGATTT
KU70-2	GATGCCCTTTACTGAAAAA
KU80-1	GAGAACAAGGATGAGATTGCT
KU80-2	CAAGCAAAGAAGGTGATAA
LIG4-1	AAGCCAGACAAAAGAGGTGAA
LIG4-2	GCTAGATGGTGAACGTATG
Scrambled	GGTCTGTACGAACCGATAGGT

Oligonucleotides used for T7EI, PCR genotyping and PCR donor generation			
Gene target	Direction	Sequence (5' to 3')	Assays
Mouse *Rosa26*	F	CGTGCAAGTTGAGTCCATCCGCC	T7EI
	R	ACTCCGAGGCGGATCACAAGCA	
Human *AAVS1*	F	TCCAGGGGTCCGAGAGCTCAGCTAG	T7EI
	R	CCAGACAGCCGCGTCAGAGCAGCTC	
AAVS1-TLR *AAVS1-GFP*	F	GGCAGCCTGTGCTGACCCATCGAGTC	
	R	CGGGATTCTCCTCCACGTCACCGCA	Genotyping
AAVS1 AAVS1-TLR	F	TCCAGGGGTCCGAGAGCTCAGCTAG	
	R1	CGGGATTCTCCTCCACGTCACCGCA	Genotyping
	R2	CCAGACAGCCGCGTCAGAGCAGCTC	
AAVS1 loading	F	CCAGGCCACCTACTTGGCCTGGAACC	
	R	CCACAGTTGGAGGAGAATCACC	Genotyping
Venus	F	AAGCTTGATTAAGCCGCCACCATGG	Donor
	R350	GTTCGTGGCCAACGCGTCTACTTGT	
	R650	CTCTCTCCCATGTGAAGCCCTCAGG	
	R950	ATAGTAGACGCCGGGCATCTTGAGG	
	R1250	GACACCTACTCAGACAATGCGATGC	